# Solar Collection of Evacuated Tubes in a Residential Electrical Power System

Undergraduate Honors Thesis

Presented in Partial Fulfillment of the Requirements

for Graduation with Distinction

at The Ohio State University

By

Michael Steven Nesteroff

Department of Mechanical Engineering

The Ohio State University

2010

| Defense Committee: | Approved by |
| --- | --- |
| Professor Yann Guezennec (Advisor) | ______________________________ |
| Dr. Shawn Midlam-Mohler | ______________________________ |

## ABSTRACT

This thesis investigates the potential of a solar thermal collection system to be utilized in a residential solar thermal Organic Rankine Cycle (ORC) power generation. The motivation behind this work is the projected rise in fossil fuel prices due to increased emission standards, fossil fuel depletion, and increasing demand in decades to come. Specifically, this study investigates the feasibility of an economically viable alternative to Photovoltaic (PV) residential electricity generation on a residential scale. Potentially, parabolic troughs, flat plat solar collectors, and evacuated tubes can serve as solar thermal collection devices. However, due to constraints linked to temperatures to be reached for feasible ORC thermodynamic cycles, the ability of functioning in diffuse sun light (cloudy conditions) and the cost associated with active solar tracking devices, the most optimal solar collection tool for residential applications is evacuated tubes. With iso-butane as a working fluid for an ORC power generation cycle, this work provides an experimental proof-of-concept that under sunny conditions, a reasonably sized residential system can be designed to produce 10 kWh of electricity. Initial tests show positive results, even though the target temperature of 90˚C was not reached for the configuration tested. Further experimental verification tests will need to be carried out under a broader range of seasonal and weather situation to give evidence that the solar collection design can indeed deliver enough energy for 10 kWh to be produced at the

target temperature required for a properly designed Organic Rankine Cycle with the proper working fluid best matched to the evacuated tube solar collection device. This work, while preliminary, provides a strong impetus to pursue this option further based on evacuated tube solar collection. In particular, future systems will need to include thermal storage, proper feedback control of the flow rate based on solar irradiation, environmental conditions and the power generation cycle energy demands and set point temperatures.

DEDICATION

This document is dedicated to my family.

ACKNOWLEDGMENTS

Professor Yann Guezennec

Dr. Shawn Midlam-Mohler

Darrin Orr

Nick Warner

Brad Engel

Jake Wither

Center of Automotive Research

TABLE OF CONTENTS

LIST OF TABLES

LIST OF FIGURES

CHAPTER 1: INTRODUCTION

## 1.1 Motivation

Generating electricity from thermal heat is no new venture. In fact most of the United States' energy is generated from burning fossil fuels (Figure 1). Currently the most cost effective means of producing electricity is by burning fossil fuels, either natural gas or coal. While this method of electricity generation proves to temporarily be cost effective, burning fossil fuels to produce electricity holds noteworthy disadvantages. These disadvantages include fossil fuel emissions, rising fossil fuel prices, and the depletion of fossil fuels. These disadvantages will be discussed in further detail to provide grounds for an alternate thermal source in electrical power generation.

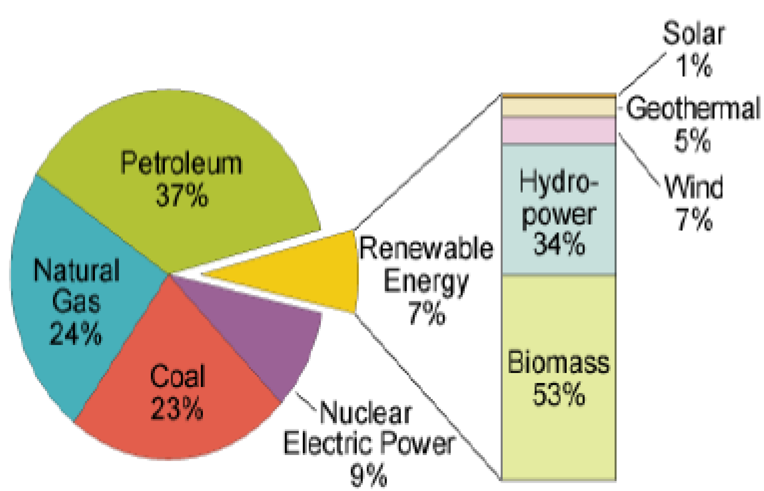


Figure 1: Energy breakdown by fuel

Many Western European countries and the United States have made a commitment to reduce greenhouse emissions by 80% by the year 2050 (Cumpsty, 2009). Reducing greenhouse emissions will prove to be a large and costly endeavor. Separating Carbon Dioxide from fossil fuel power plants is estimated to have ‘about a 9 percentage point loss in overall plant efficiency with an increase in electricity cost of about 44%’ (Cumpsty, 2009). As the world moves towards producing clean energy, this extra cost burden will be placed on the customer. Previously, renewable clean energies may have been costly, but as power companies eliminate greenhouse gas emissions, renewable power sources will become more cost effective and even competitive. With the reduction of greenhouse emissions, alternate thermal sources for Rankine Power Cycles must be explored.

A worldwide increase in energy demands will drive the price of fossil fuels higher. Figure 2 shows consumption of all fuels to have an increasing trend over time. Emerging markets such as China and India will demand more fuel as their energy needs increase. With emerging demand, the prices of fossil fuels will inevitably increase. While coal is abundant and cheap, if high population countries like China and India fully industrialize, this may lead to an increase in the cost of coal. With a worldwide demand for more energy, new avenues of energy production must be explored. The economic climate yields a potential for fluctuating fossil fuel prices. Unstable fossil fuel prices will open the market for sustainable alternative energy. The world needs alternatives to fossil fuels.

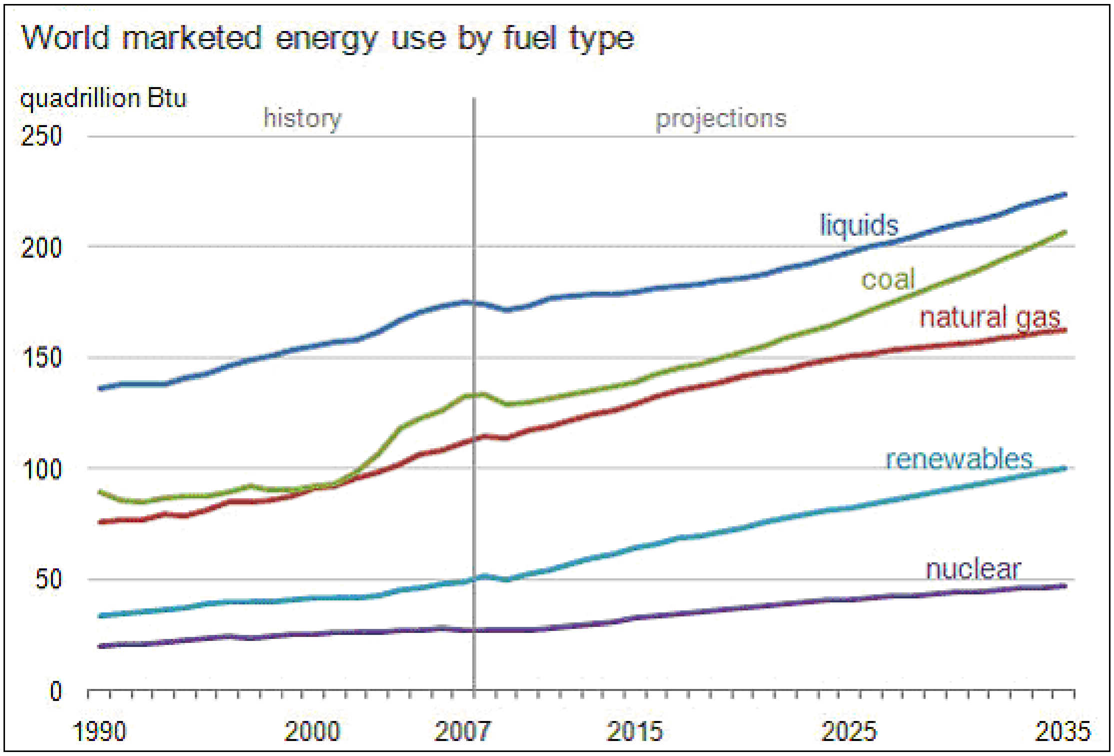


Figure 2: United States Energy Information Administration (EIA) World Market Energy Outlook (Department of Energy, 2010)

There is a limited supply of fossil fuels. While the world market for energy is projected to increase over time, fossil fuel production is expected to decrease in the future. The production of oil worldwide is expected to decrease this decade of 2010 (Korpela, 2002). The peak production of other fossil fuels like coal and natural gas is less certain, but is looming in the distance. Figure 3 shows the projected peak production of oil and natural gas. As fossil fuel production decreases there will be less supply available to meet the increasing demand of the world market. This will drive up the price of energy. With this ensuing economic climate, the market for alternative energy will become more profitable.

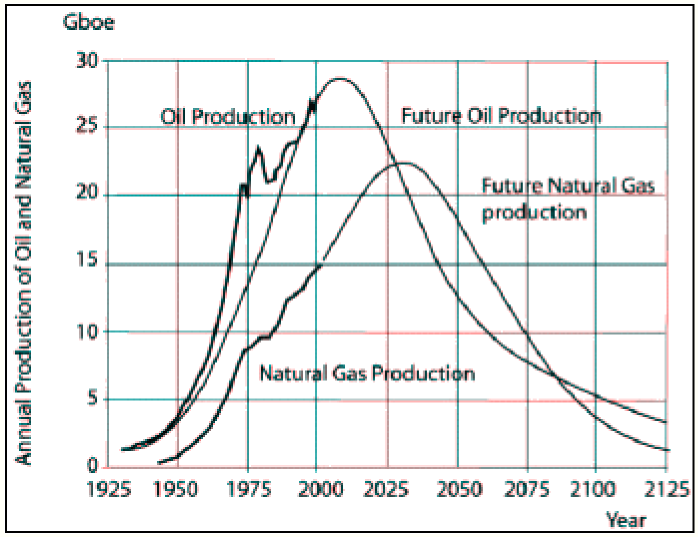


Figure 3: Peak oil and natural gas projected curves (Laherrere, 2001)

Much capital has been invested in renewable energy in recent times. Since 2003 the National Renewable Energy Laboratory (NREL) has assisted the renewable energy industry in raising $3.4 billion (National Renewable Energy Laboratory, 2010). Huge solar and wind farms are being constructed in many different states. Figure 4 shows cities in America using solar power in grid applications. The Department of Energy (DOE) states that “domestic growth (for solar energy) is also increasing as a result of the state incentives and federal tax incentives for residential and commercial use.” Residential solar has become a pronounced market of late. In 2001 ‘Home Depot began selling residential solar power systems in three of its stores in San Diego, California. A year later it expanded its sales to include 61 stores nationwide (Solar Timeline, 2010).’

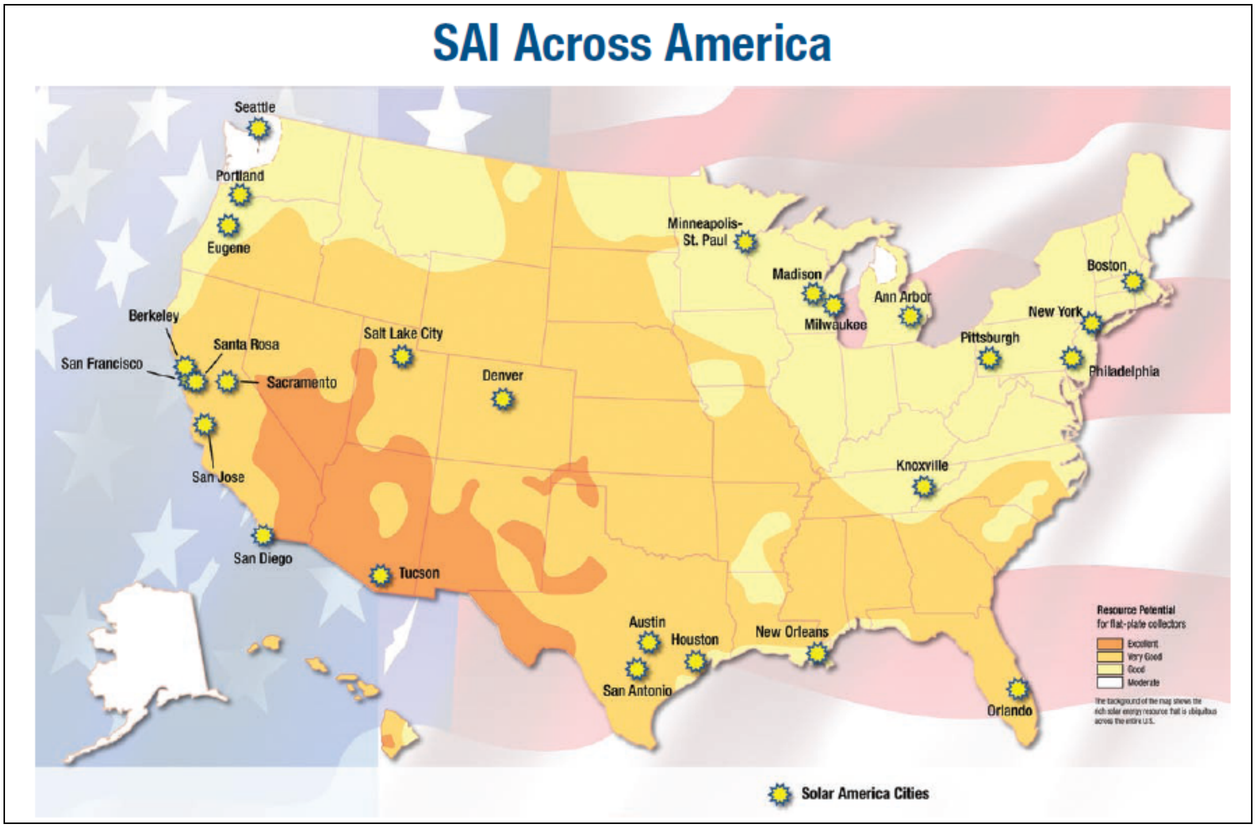


Figure 4: American cities using solar energy in grid applications (DOE)

There is high potential for solar power to be utilized in the United States. Figure 4 shows that most of the United States is optimal for solar power production. Currently there are two ways of harvesting solar energy, photovoltaic technology and solar thermal technology. Photovoltaic cells collect sun rays, directly converting the energy into electricity. The problems with photovoltaic cells include only achieving efficiencies of typically 10%, producing no electricity at night, and not being very cost effective producing electricity at $0.30 kW-hr (Quaschning, 2001). However, First Solar, Inc. has recently reached a milestone in manufacturing photovoltaic cells at $1/Watt (First Solar, Inc., 2009). This is three times less expensive than manufacturing costs in 2004 being

$3/Watt (First Solar, Inc., 2009). If photovoltaic cells continue to become more cost effective, their use on a residential scale will become more pronounced.

On the other hand, solar thermal power plants have operated on an industrial level since 1984 (Quaschning, 2001). Industrial solar thermal power plants installed in 2001 averaged $0.12-0.14 kW-hr, more than half the cost for electricity generated by photovoltaic cells (Quaschning, 2001). The potential for solar thermal power production is very exciting. If one percent of the Sahara Desert was covered with solar thermal power plants, the electricity could power the world (Quaschning, 2001). Solar thermal power plants can run at night and in bad weather off of stored thermal heat or from an additional furnace. The solar thermal power plant in Figure 5 has a furnace for such occasions. The only disadvantage of solar thermal concentrators is that they can only capture heat in direct sunlight. When sunlight is diffused in cloudy conditions, concentrating sunlight with mirrors becomes impossible. For this reason solar thermal power plants are optimal only for locations with high exposure to direct sunlight.

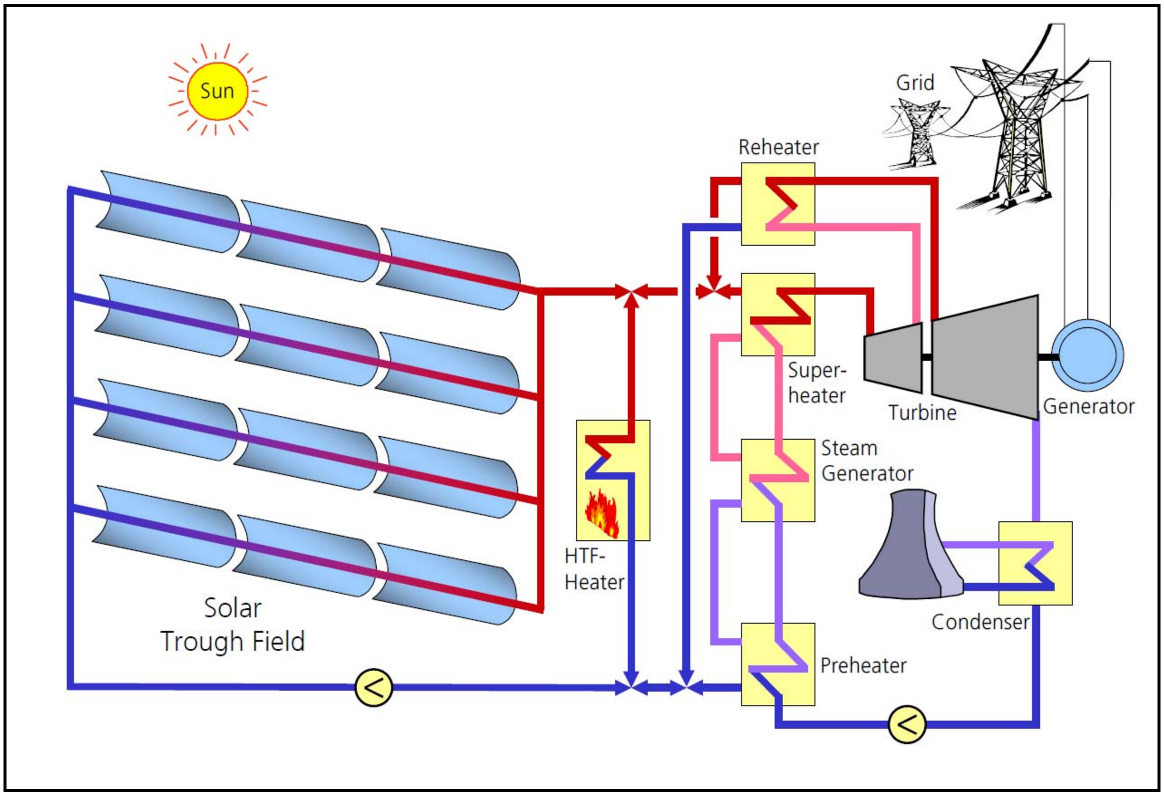


Figure 5: Solar thermal industrial power plant (Quaschning, 2010)

There are two solar collection apparatuses used in solar thermal power plants, solar parabolic troughs (Figure 6) and solar heliostat mirror concentrating towers (Figure 7). Figure 5 shows an example of the layout of a parabolic concentrating power plant. Parabolic trough technology can reach temperatures up to 400˚ C; while heliostat mirror concentrating towers can reach 1000˚ C (Quaschning, 2001). These solar concentrators are used in industrial scale power production on the order of 10-100MW (Figure 8). These large solar collectors track the sun during different seasons and times of day. They operate over large surface areas to precisely concentrate the sun's solar rays creating enough heat to drive a Rankine power cycle. With all of this being said, the industrial solar power plant would be quite difficult to scale down on a residential level.

Figure 6: Parabolic trough solar concentrator (Florida State University, 2010)

Figure 7: Heliostat mirror concentrating tower solar concentrator (E-solar, Inc., 2010)

There is an absence of solar thermal power plants on a residential level ranging from 1-3 kW (Figure 8). The absence is mostly due to the fact that solar thermal power production relies on direct sunlight and solar tracking. The expense of solar tracking for an output of only 1-3 kW is a high cost. This expense is compounded because the solar power plant will only be effective during completely sunny days. However developing a residential solar thermal power plant would be very feasible, if a solar collector exists that does not need a solar tracking system and can operate in diffused sunlight.

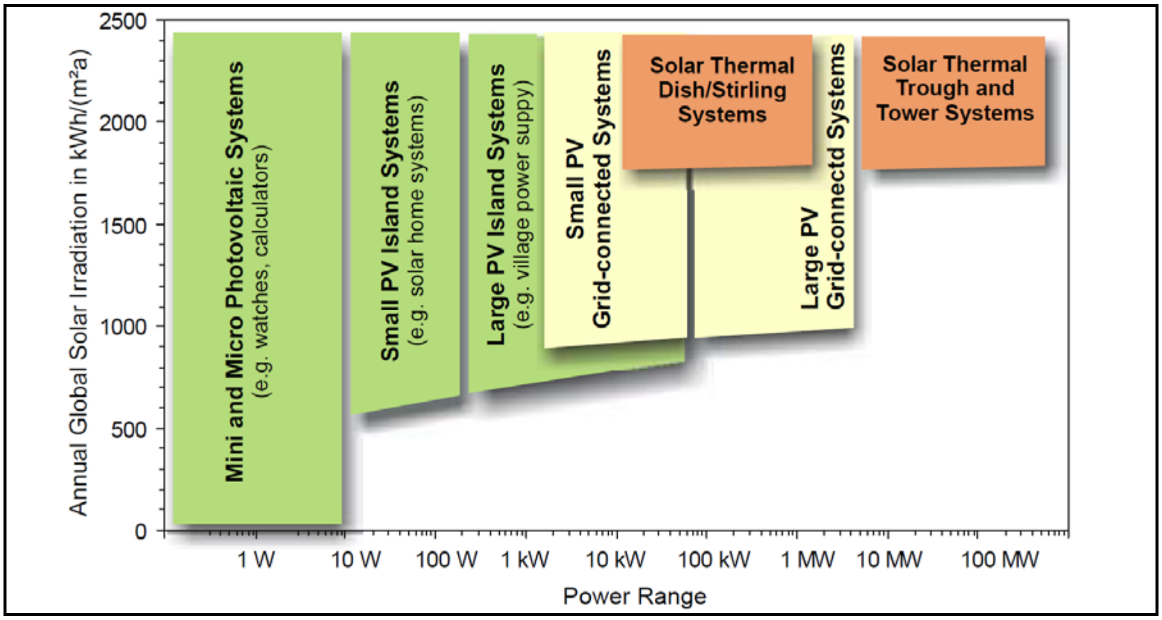


Figure 8: Solar industry breakdown by plant power range (Quaschning, 2001)

Residential solar thermal technology can provide electricity and heat, potentially reaching a higher overall efficiency compared to photovoltaic cells. The heat collected from the solar collector will drive a Rankine power cycle, generating electricity. After electricity generation, the exhaust heat from a solar thermal system could be used to preheat water or power a heat pump to help heat or cool a home. Solar thermal is a versatile technology which on a residential scale has the potential to supply the home with most of its energy needs.

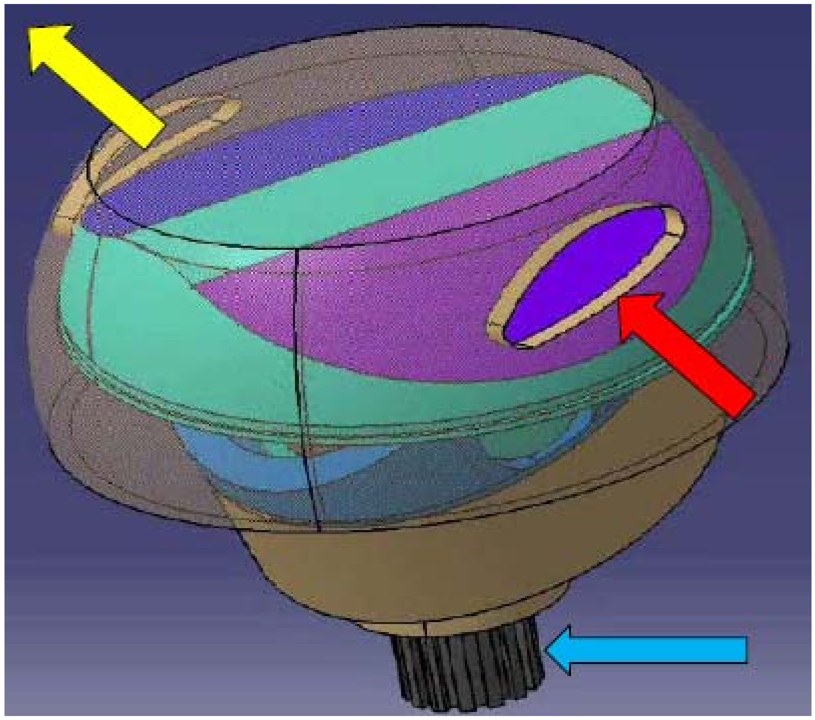

Figure 9: Expansion device being developed by The Ohio State University

## 1.2 Thermodynamic Cycle

Solar thermal power plants are thermodynamic cycles driven by a change in temperature and pressure. For instance, steam power plants use a boiler to generate water vapor. At this point the steam is at a high energy level with an elevated temperature and pressure. The high energy steam is expanded in a controlled manner through a turbine. The energy is transferred using the turbine. Downstream of the turbine is a low energy state, low temperature and pressure. Because of the second law of thermodynamics, the high pressurized vapor will move downhill to a low energy state. Figure 10 displays a basic thermodynamic steam power cycle in a T-S diagram. The water is heated until vaporized and heated to a superheated state. The superheated steam drops to a low energy state as seen in the T-S diagram. The difference between the states S1 and S2 describes the work of the turbine. The two different states are characterized by different temperatures and pressures. The larger the difference between the temperatures and pressures, the more work the system can generate.

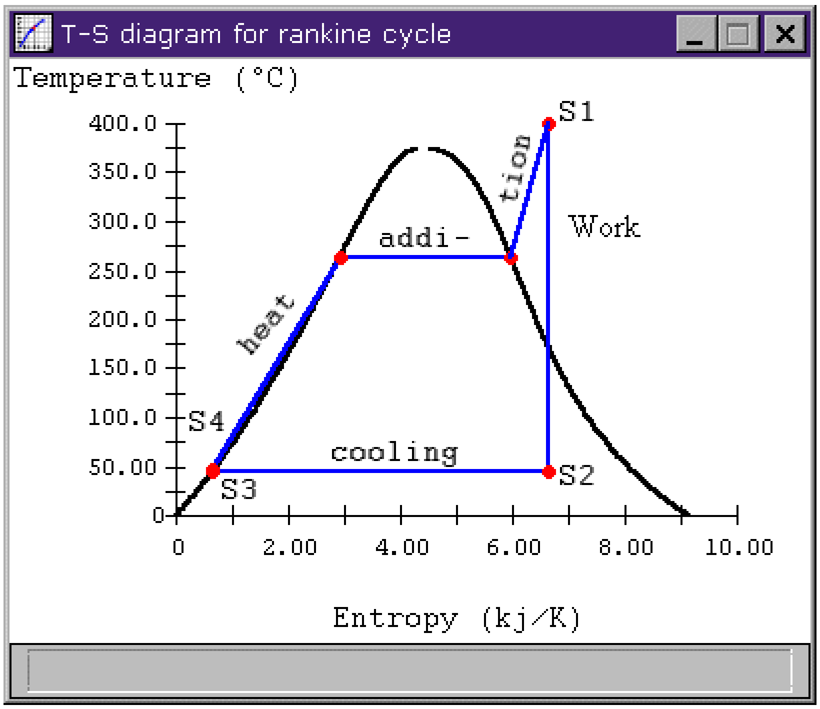


Figure 10: Thermodynamic Power Cycle (Northwestern University, 2010)

An expander device is being developed by an Ohio State, which can run at a couple kilowatts, replacing a turbine in a Rankine power cycle (Figure 9). The expander is designed to be used in a residential solar thermal power plant application. To maximize the work of the expander in the residential power system, the same principles apply as in the steam thermodynamic power cycle. From Figure 10, increasing the residential power system's performance requires increasing the pressure difference between the hot and cold states. In order for the residential power plant to be developed the evacuated tubes must collect enough energy with a large temperature difference so that a Rankine power cycle can run efficiently. The cold state is defined by ground water temperature. Since the low temperature is fixed, the high temperature becomes the limiting factor. High temperatures will yield large work outputs.

## 1.3 Solar Collection

There are a few solar collection technologies on the market today suitable for a residential solar thermal power plant. These technologies include parabolic troughs, flat plat collectors and evacuated tubes. The pros and cons of each solar collection method will be explored, and the technology that best fits a residential power plant will be chosen.

Parabolic troughs have been briefly discussed already and can be seen in Figure 6. This technology uses parabolic geometry to focus the sun's radiation to a focal line. As stated before, parabolic troughs can reach temperatures up to 400˚ C. A residential parabolic trough would not be as large as an industrial parabolic trough. Therefore since the concentrating area would be smaller for the residential parabolic trough, it would not be able to reach temperatures of 400˚ C. However, a residential parabolic trough would still be able to reach high temperatures. The cons for this technology are, needing direct sunlight, needing a solar tracking system, and being large and bulky. The biggest strike against solar concentrating troughs is the fact that they only can operate in direct sunlight. This technology would not operate well in places like the Midwest, where cloudy weather can continue for weeks. Parabolic troughs are a viable option for a residential power plant, but there may be more viable options.

Solar thermal collecting plates as seen in Figure 11 are a low cost way to capture heat from the sun. These solar collection plates are already on the market, but used for water and home heating. The solar collection plates work best in direct sunlight, but also can collect heat from the sun in diffused sunlight. The downside to flat plat collectors is that they have high heat losses, so they cannot reach high temperatures. In most cases flat plate collectors reach temperatures of 50-60 ˚C, which is well below where a solar thermal power plant would run. Because of this, flat plate collectors are not a viable option in designing a residential solar power plant.

Figure 11: Solar Flat Plate Collectors

Evacuated tubes are a versatile technology which are very similar to flat plate collectors, but without the major heat losses. Evacuated tubes are currently on the market for home heating applications (Figure 12). Evacuated tubes can reach temperatures of 300 degrees Fahrenheit according to a manufacturer's report (Silicon Solar, 2010). The goal of solar collection is to capture as much energy as possible at the highest temperature possible. The higher the temperature range is, the more efficient the system can be. Since evacuated tubes can operate in diffused sunlight, are low cost, and can reach high temperatures, these collectors are ideal for a residential thermal power plant.


Figure 12: Evacuated solar tubes

Solar evacuated tubes are very efficient thermal collectors. Evacuated tubes are encompassed by a glass surface. Beneath the glass is a vacuum layer, which acts as insulation. The vacuum surrounds a heat pipe coated with a black radiation absorbing finishing. The sun's radiation travels through the glass and through the vacuum layer and strikes the heat pipe. The heat pipe absorbs the sun's radiation, resulting in a thermal energy transfer. As the heat pipe is exposed to radiation, the heat pipe transfers the heat to the tip of the pipe (Figure 13). The tip is connected to a manifold, which acts like a heat exchanger. A heat transfer liquid in the solar collection loop passes through the manifold and heats up via convection from the heat pipe. There will be many evacuated tubes in series, so as the heat transfer liquid passes by each tube, the liquid is heated (Figure 14).

The weather, flow rate of the heat transfer liquid, and the amount of tubes in series determines the effectiveness of the solar collection of evacuated tubes.

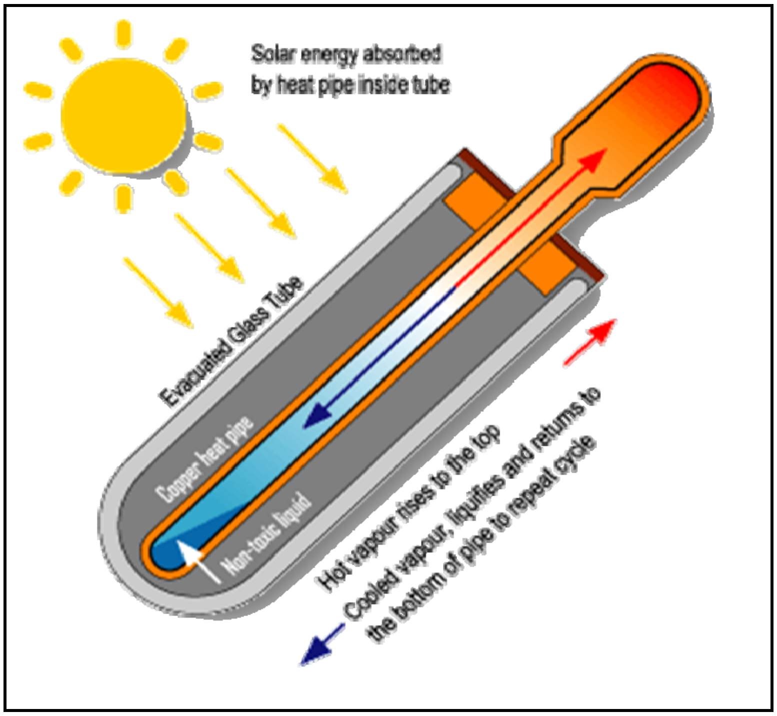


Figure 13: Solar evacuated tube layout

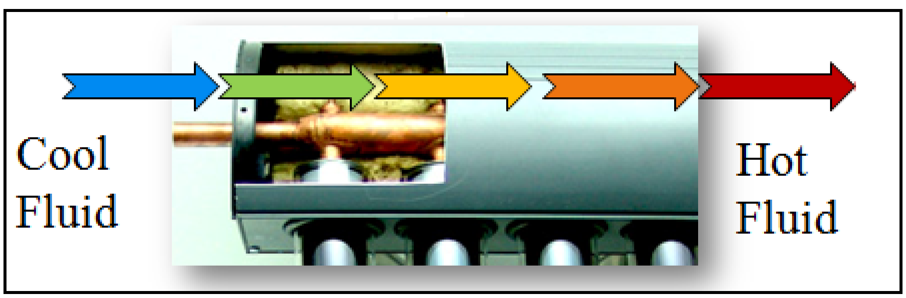


Figure 14: Convection across solar evacuated tubes

To increase the temperature capacity of the solar evacuated tubes, a parabolic solar concentrator will be added to the system. The trough will use parabolic geometry to concentrate solar radiation to a single evacuated tube. The solar concentration will provide the tube with intense radiation. From the intense radiation, the tube will reach higher temperatures. Another way to increase the temperature of the solar tubes is to place a reflective surface behind the panel of tubes. The surface will reflect light that passes through the tubes. Instead of being lost the light will now have a second chance to be absorbed by the evacuated tubes. These two improvements will be tested to see how effective they are to the solar collection system.

Direct sunlight provides about 1 kW per square meter, but fluctuates depending on where the sun is in the sky. The average residential home in the United States uses 936 kWh a month (Department of Energy, 2010). This means that an average of 1.3 kW’s is needed to power a typical home. But to create a thermal power plant capable of producing a few kW’s of power efficiently, a high temperature range must be obtained by the solar collectors. The system’s theoretical efficiency is bound by the temperature displayed in the Carnot Efficiency Equation (1.1). The larger the temperature difference, the more efficient the system can be. Since the ground water temperature on average is 10 °C, this is the equation’s lower bound. To reach high system efficiencies, high temperatures will needed. Figure 15 shows the Carnot efficiencies on the y-axis for a given temperature range seen on the x-axis. To reach high temperatures, the solar collectors must concentrate sunlight to make the sunrays more intense. This is known as solar concentration, which can be compared to burning an ant with a magnifying glass.

The magnifying glass concentrates direct sunlight over a large area to a smaller area, resulting in intense heat. If the target plant efficiencies are 20-25%, a theoretical minimum of 100-150 °C must be reached (Figure 15).

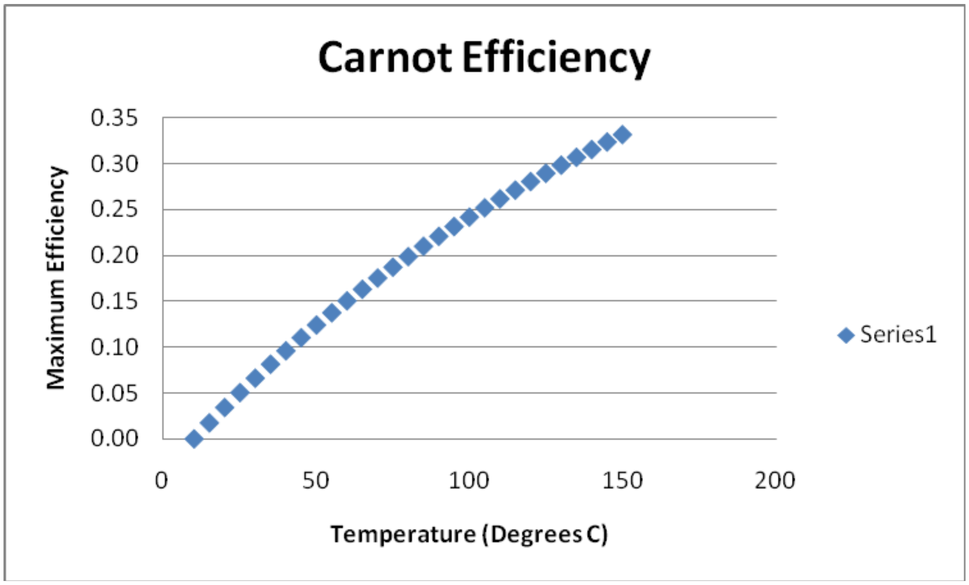


Figure 15: Carnot Efficiency for given temperature range

$$\text{Carnot Efficiency} = \frac{T_H - T_C}{T_H} \quad (1.1)$$

The power capacity of the solar tubes will determine the power capacity of the residential power system. But in order to design a solar collection system, the amount of solar radiation available must be determined. The National Renewable Energies Laboratory (NREL, 2010) has gathered solar data for thirty years. The NREL has developed a program which generates the average solar radiation for the United States, given a month and the type of solar tracking. Solar tubes use a north-south tilted axis tracker. Figure 17 through Figure 24 display solar irradiance maps of the United States and plots of daily irradiance taken from Golden, Colorado during the four seasons.

To get kW per meters squared of radiation during sunlight hours, divide the values in Figure 16 by the amount of sunlight hours during a particular day. A typical October Ohio day from sunrise to sunset is about eleven hours. Of these eleven hours eight may be optimal for solar collection. An average of 3.5 kWh per square meter per day can be collected in October in Ohio. When dividing the 3.5 by 8 hours, an average of 0.44 kW per square meter of power can be collected. Therefore as tests are carried out in October, an average solar irradiance is expected to be 0.44 kW per square meter.

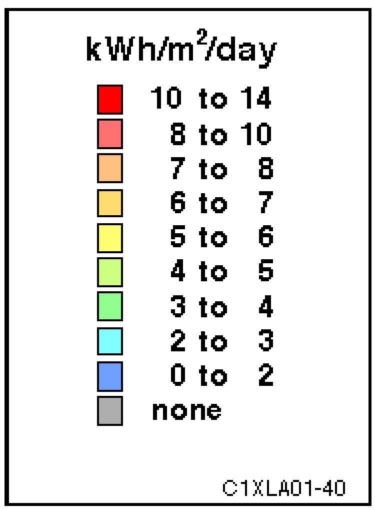


Figure 16: Radiation grid for solar maps

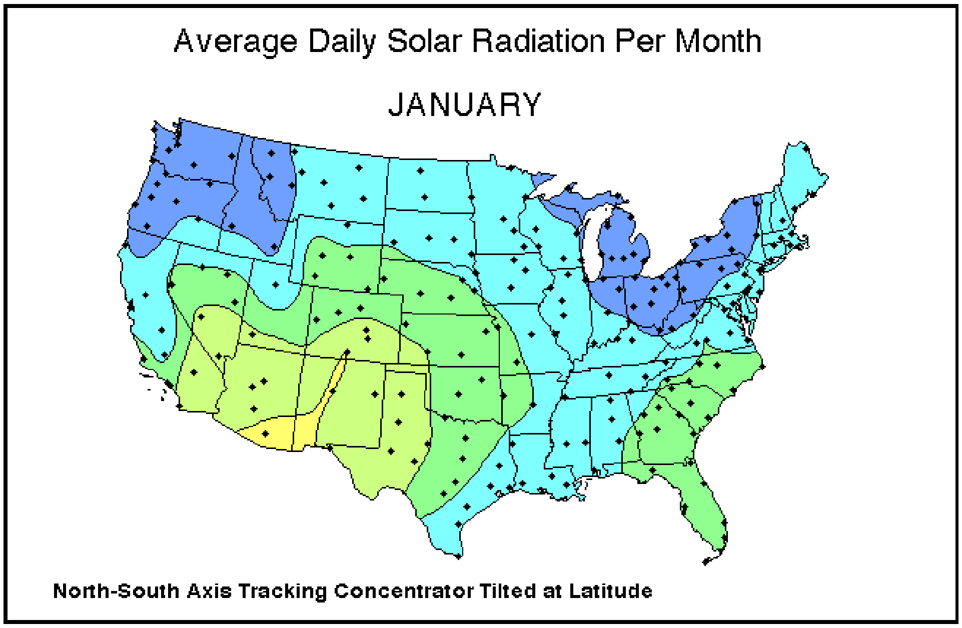


Figure 17: Average solar radiation map for a North-South tracking concentrator in January.

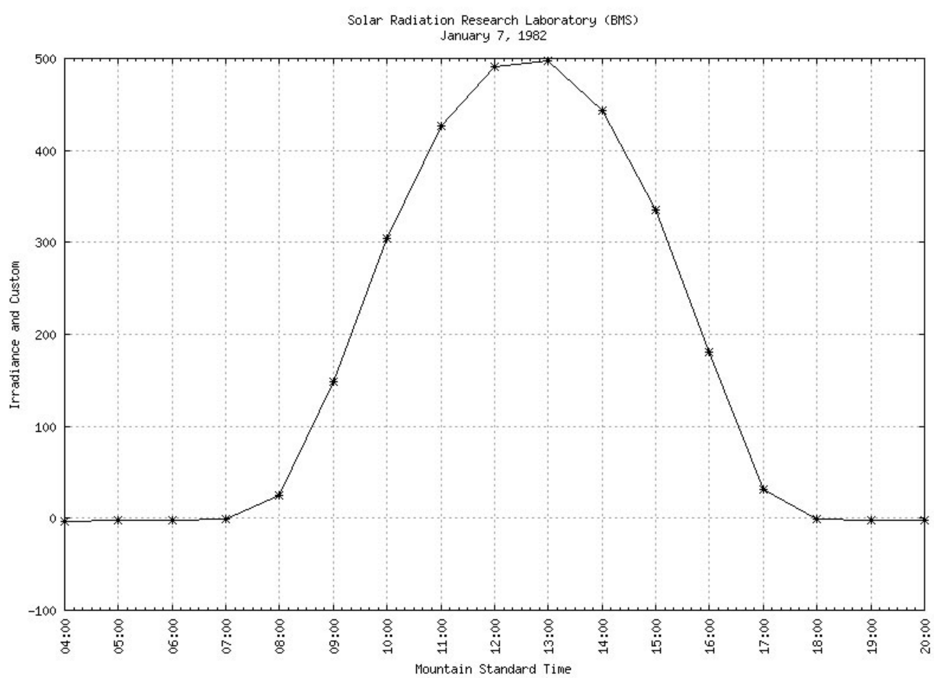


Figure 18: Solar Irradiance in Watts for a sunny January day in Golden Colorado

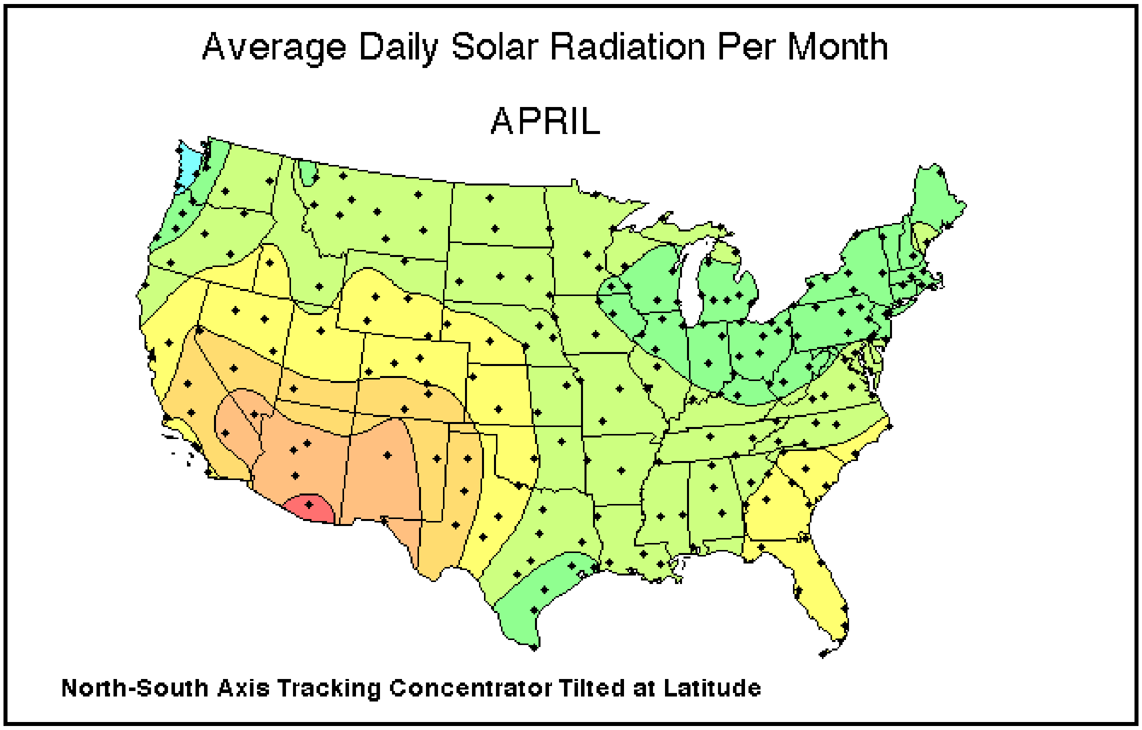


Figure 19: Average solar radiation map for a North-South tracking concentrator in April.

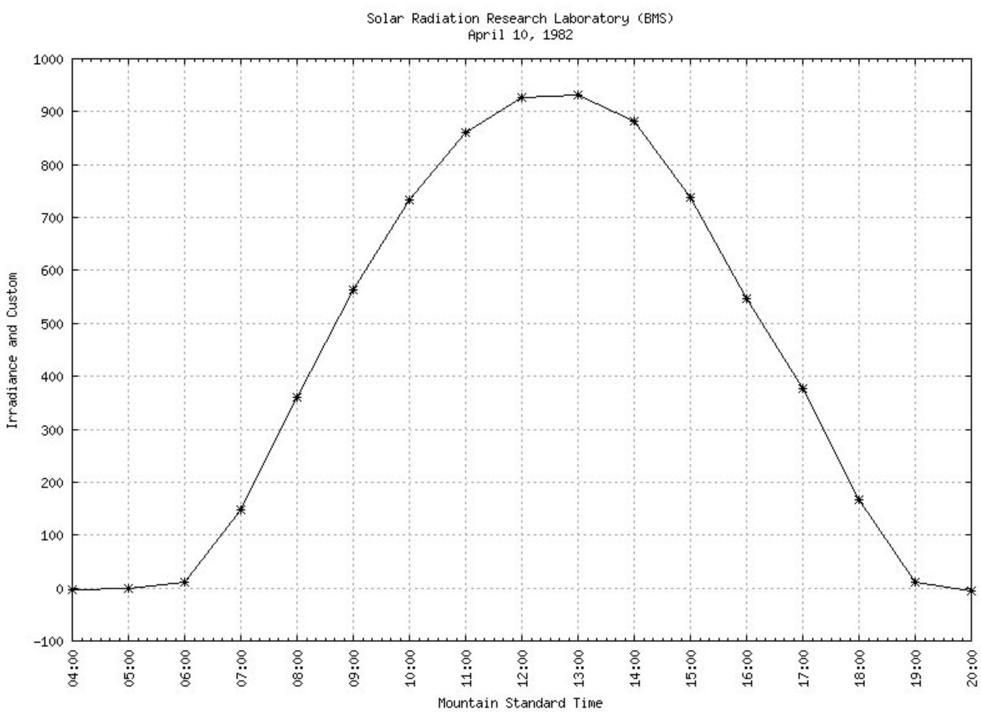


Figure 20: Irradiance in Watts for a sunny April day in Golden Colorado

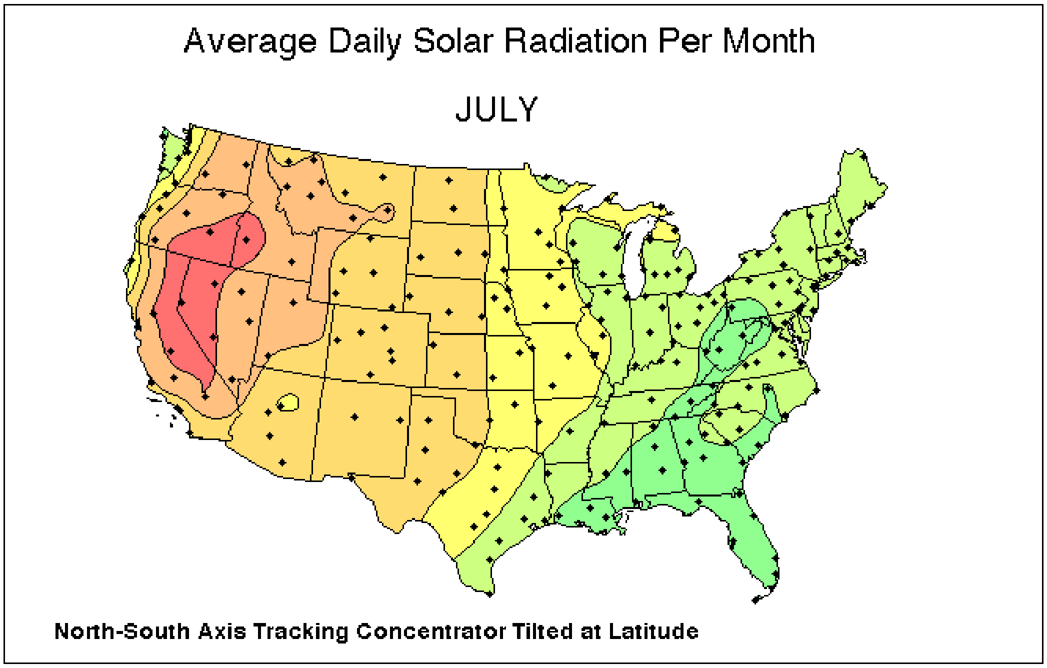


Figure 21: Average solar radiation map for a North-South tracking concentrator in July.

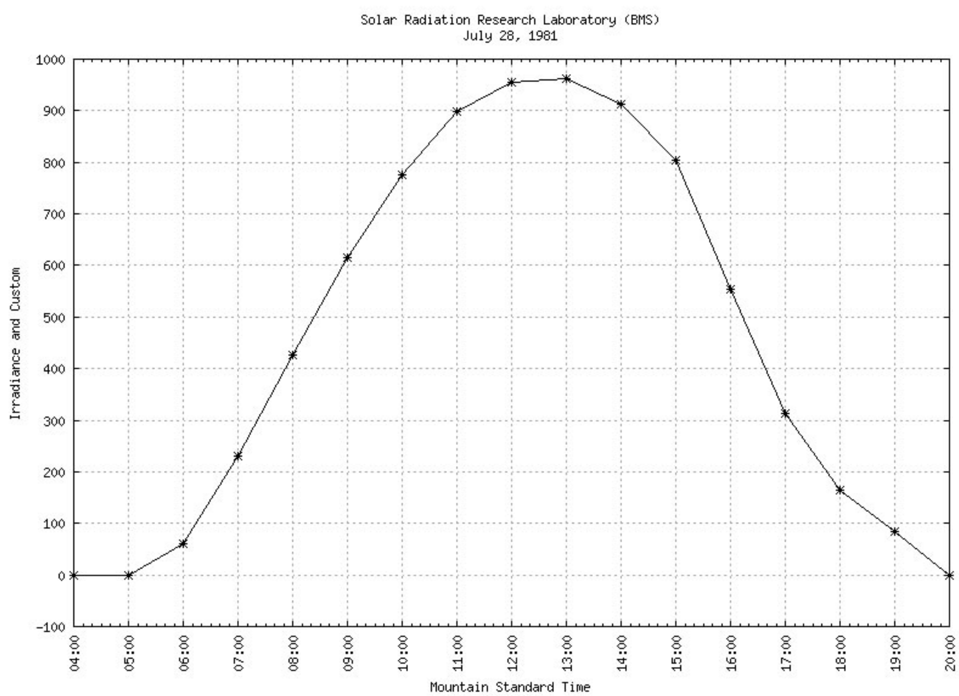


Figure 22: Irradiance in Watts for a sunny July day in Golden Colorado

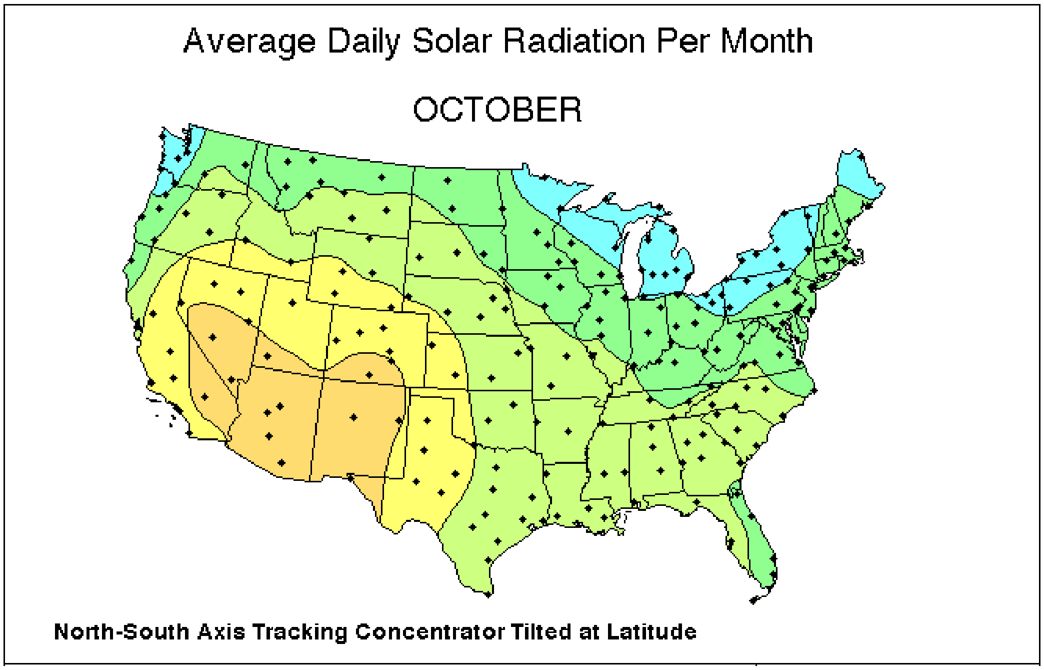


Figure 23: Average solar radiation map for a North-South tracking concentrator in October.

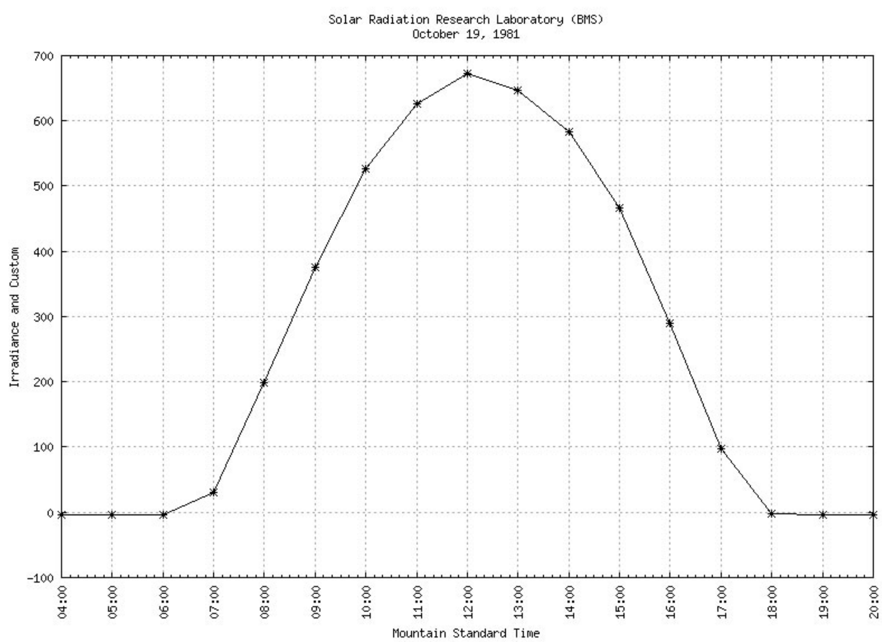


Figure 24: Irradiance in Watts for a sunny October day in Golden Colorado

From the irradiance plots there is a clear difference between July and January irradiance. The January peak is at 500 W, this is half of the July's peak. The solar power system will struggle during the winter months. The following chapters will determine whether it is feasible to produce electricity during the winter months or if the thermal energy captured should be used for residential heating applications. There is potential for solar power in every month. The following chapters will lay out a plan to harness the energy from the sun and develop a system to provide both electricity and heat for residential applications.

## 1.4 Project Overview

Testing the solar thermal collection parameters of the residential power station are critical because the solar heat collected provides the input energy to the thermodynamic power cycle. The parameters to be investigated are maximum temperature, solar collection capacity in Watts per meters squared, and the thermal efficiency of the system. In addition, a solar concentrator will be added to the system to determine if concentrated solar light provides an increase in performance.

To meet the electrical power needs of residential consumers, a solar thermal electrical power system is being developed (Figure 25). This electrical power system operates purely off of the sun's radiation. The system will consist of two closed loops. One loop will be the solar collection loop, gathering heat from the sun (1 Figure 25). The other loop will be the power cycle, converting the captured solar heat into electrical energy. The loops will be separate and will transfer heat through a heat exchanger. The heat exchanger will reside inside of a storage tank. This tank will store the collected heat from the sun throughout the day. Evacuated tubes will be used as solar collectors to capture heat from the sun. A heat transfer liquid will pass through the evacuated tubes, and gather thermal energy through convection. This energy is then transferred and stored in a heat storage tank. The storage tank will also act as a boiler over in the power cycle loop. The power loop consists of a refrigerant liquid which evaporates at moderate temperatures. As the refrigerant passes through the storage tank's heat exchanger, the refrigerant vaporizes (2 Figure 25). The high pressure, high temperature vapor is full of energy. The vapor is dispensed into an expander device which rotates as the vapor passes through to a lower energy state (3 Figure 25). The expander is attached to an electrical generator. As the expander spins the generator converts the kinetic energy into electrical power (4 Figure 25). The system will be capable of producing 1-2 kW of electrical power.

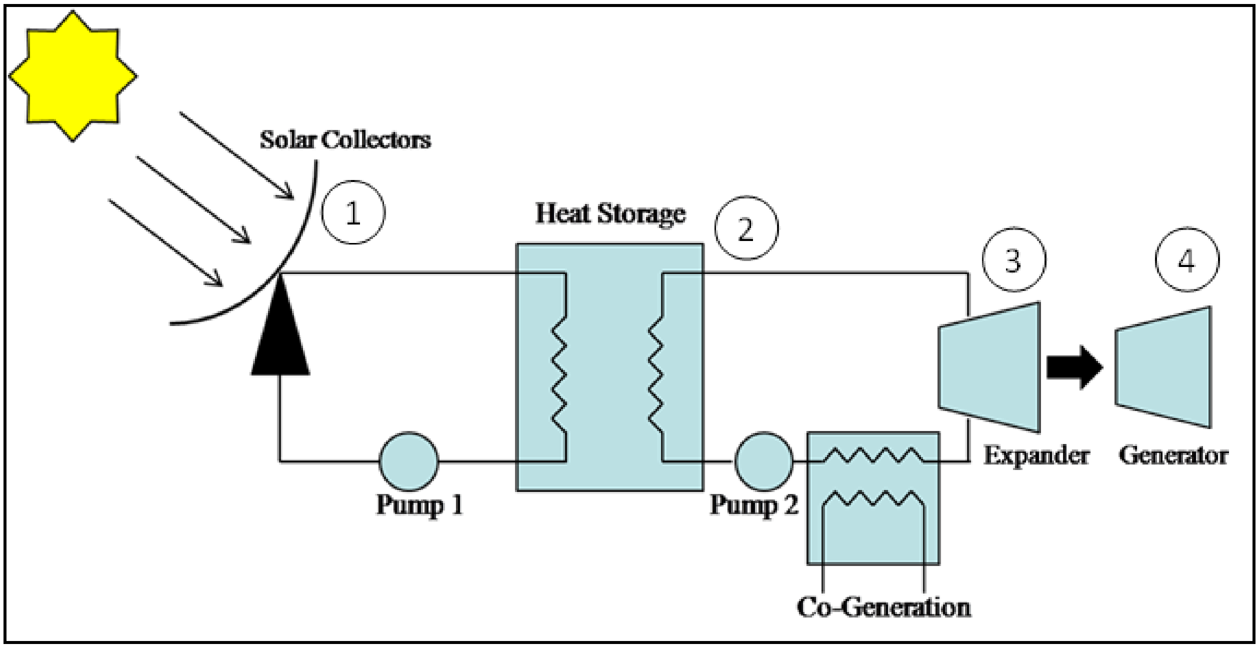


Figure 25: Residential solar thermal overview

The overall objective is for the system in Figure 25 to produce 2 kW of electricity. To accomplish this much more heat must be collected by the solar collection loop. The solar energy must be collected within a 90 square meter foot print, which is the typical dimension of a roof. The solar collection system must reach high temperatures of at least 90 °C, for this is the temperature a low temperature Rankine cycle can run. Table 1 summarizes the goals for this project.

Table 1: System objectives

| | |
|---|---|
| Electrical Power | 2 kW |
| Solar Collection Area | < 90 square meters |
| High Temperature | > 90 °C |

# CHAPTER 2: THEORETICAL ANALYSIS AND DESIGN

## 2.1 Introduction

The following chapter uses data from the manufacturer to design a solar collection system with evacuated tubes which meets the objectives listed in Table 1. The system will be designed with isobutane as the working fluid. The chapter will reveal that designing a residential solar system to generate 2 kW electricity in cloudy conditions and during the winter is not feasible. Rather the solar collection system shall be designed to collect enough thermal energy to power the 2 kW system in sunny conditions. During cloudy weather or winter months, the solar system shall be used for home heating exclusively.

## 2.2 Isobutane as Working Fluid

J. Wither (2010) has completed a performance analysis of isobutane in a residential Rankine Power cycle as shown in Figure 25. When isobutane is pressurized to about 16 bar, the fluid evaporates at 90 °C. Evacuated Tubes are easily able to deliver temperatures of this magnitude. With Jake’s performance analysis and data from the manufacturer, a solar collection system can be designed to deliver 2 kW of electricity with isobutane as the power cycle fluid.

The performance of the thermodynamic cycle largely depends on the pressure ratio the expansion device in Figure 9 can reach. The expander has not been completely developed, but similar technologies suggest a reasonable estimate for expansion is a pressure ratio of eight. Assuming ground water is about 15 °C, the vapor dome for isobutane can be defined as in Figure 26. Figure 26 suggests that super heating isobutane could enhance the power output of the system. However, Jake Wither has performed research that shows there is no added benefit to super heat isobutane. Therefore there is no added benefit to heat the isobutane over 90 °C. The power generated from the expansion device comes from the drop between saturated vapor at 16.4 and 2.5 bar.

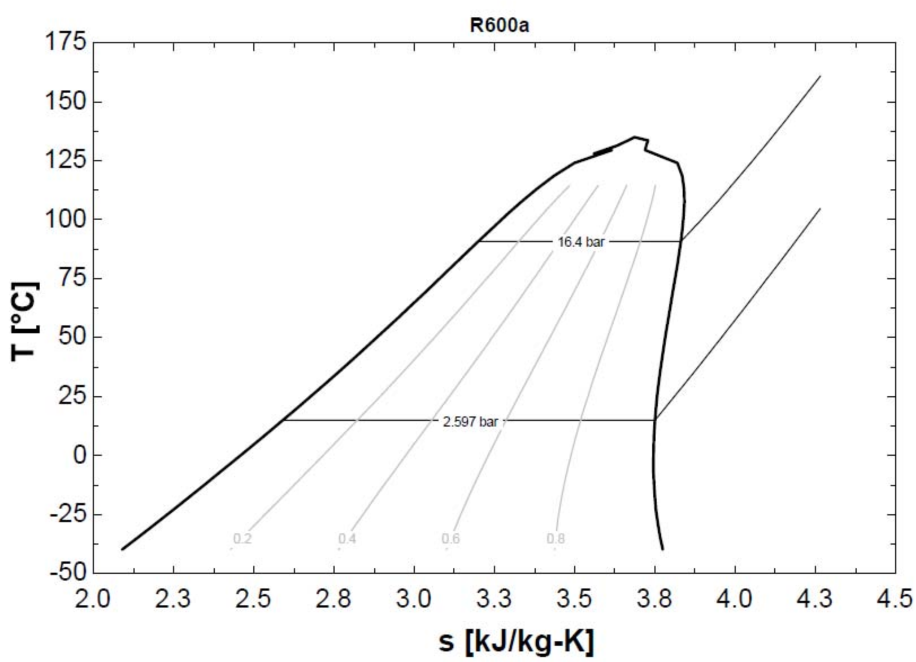


Figure 26: Vapor dome of isobutane

J. Wither has run simulations to yield that the overall efficiency of a residential power system is 12.6 % operating under the defined conditions in Figure 26. Figure 27 suggests that if higher temperatures and pressure ratios can be reached, a higher efficiency will also be reached. Evacuated tubes are capable of exceeding 90 °C, but since the expansion pressure ratio has not been solidified and because the project is in the development stage, a conservative system efficiency of 12.6% has been chosen. The system efficiency can be used to design a solar collection system to deliver 2 kW of electricity. The solar collection temperature must exceed 90 °C to account for losses in the heat exchanger. For this theoretical calculation, these losses will be neglected, so 90 °C will be the target solar collection temperature.

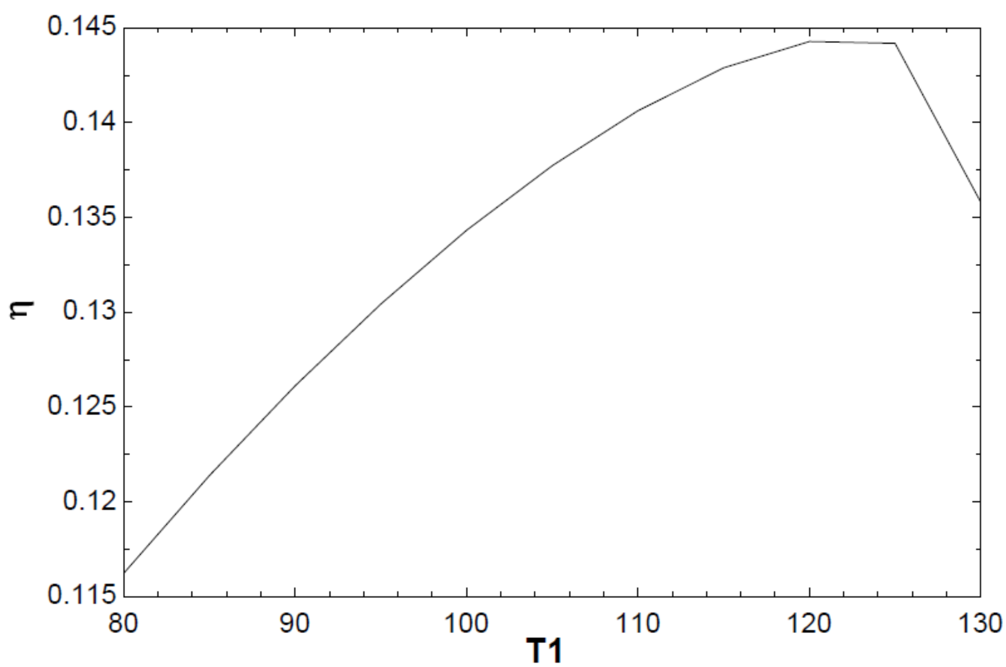


Figure 27: Efficiency as a function of temperature in degrees Celsius

## 2.3 Solar Collection Design Utilizing Manufacturer's Data

Dividing the desired 2 kW electricity by the system efficiency of 12.6%, will yield the needed thermal power of about 16 kW. To design a solar collection system that can generate 16 kW of thermal power, data from the Fraunhofer Institut will be used regarding the performance of the evacuated tubes. The tests from the Fraunhofer Institut were completed according to standard EN 12975-1,2:2006. The test completed by Fraunhofer was to determine the thermal output power of the evacuated tubes. Tests were accomplished under varying levels of radiation, with differing changes in temperatures across the tubes. The notation Fraunhofer uses for different temperatures are defined below.

$t_{in}$ = collector inlet temperature (°C)
$t_e$ = collector outlet temperture (°C)
$t_a$ = ambient temperature (°C)

$$t_m = \frac{t_e + t_{in}}{2}$$

The Fraunhofer Institute used the model Sunmaxx-30 to complete the thermal power output test. The Sunmaxx-30 is a panel of 30 evacuated tubes with an aperture area of 2.79 meters$^2$. Figure 28 shows the power output for the Sunmaxx-30 with respect to change in temperature across the panel of tubes for a perfectly sunny day with irradiance of 1000 W/m$^2$. Figure 28 shows that for larger temperature differences between mean temperature and the ambient temperature of the Sunmaxx-30, the solar collection efficiency decreases. Therefore when the evacuated tubes reach high temperatures, they do not produce as much power as they would at lower temperatures. However, the residential electricity generating system uses the Carnot Efficiency to determine the theoretical system efficiency. The Carnot Efficiency increases with an increase in temperature. Somewhere there is a trade-off between the heat losses in the evacuated tubes, and the benefit of having high temperatures in a Rankine cycle. This trade-off will be better understood in the future when a complete prototype is running.

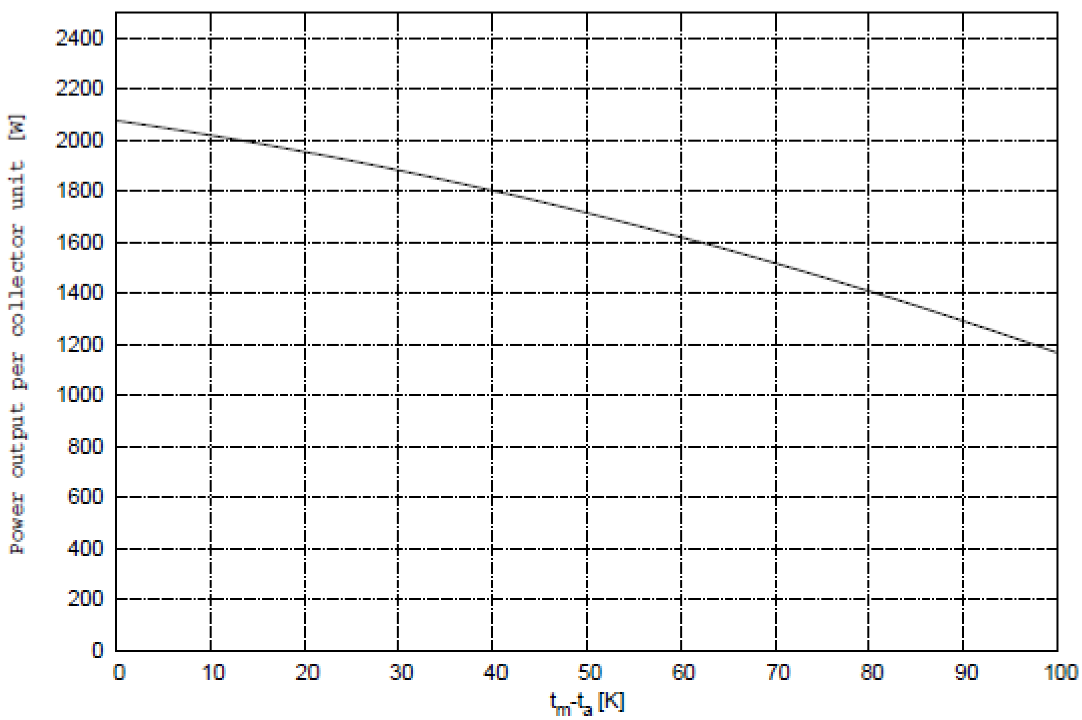


Figure 28: Power output for Sunmaxx-30 with 1000 W/m$^2$ radiation

In order to determine how many tubes are needed to supply 16 kW thermal, the system temperatures must be defined. The high temperature desired is known to be 90 °C. Anticipating heat losses an evacuated tube exit temperature of 100 °C is desired. The inlet temperature is assumed to be 20 °C. Ambient temperature is also assumed to be 20 °C. Therefore the mean panel temperature is 60 °C, and the difference between the mean and ambient temperatures is 40 °C. Under these conditions, Figure 28 shows that the thermal power for a Sunmaxx-30 is 1800 W. This means about 9 Sunmaxx-30 panels are needed to deliver 16 kW thermal. For tabulated results see Table 2.

Table 2: Evacuated tube design for 1000 W/m$^2$

| | |
|---|---|
| Thermal Output Power kW | 16 |
| Gross Area m$^2$ | 50 |
| Aperture Area m$^2$ | 25.1 |
| Number of Evacuated Tubes | 270 |

It is unrealistic to assume that the sun is going to shine at 1000 W/m$^2$ irradiance all the time. For this reason the system should be designed to deliver 16 kW thermal under cloudy conditions defined as 400 W/m$^2$. For irradiance of 400 W/m$^2$ the Fraunhofer Institute has given three data points presented in Figure 29 and Table 3. Figure 29 exhibits the same trend as Figure 28 providing confidence in the trend line added to the figure. At 400 W/m$^2$ irradiance and all other temperatures the same as above, the thermal output power per panel is 570 W. To find the amount of panels needed, divide 16 kW by the 0.57 kW each panel can produce. It takes about 28

Sunmaaxx-30 panels to produce the 16 kW thermal. 28 Sunmaxx-30 panels results in 840 evacuated tubes, 155 square meters of gross area costing $16,800 just for the tubes. Table 4 shows the listed results. The solar collection system cannot efficiently produce 16 kW of power at irradiance of 400 W/m$^2$.

Table 3: Sunmaxx-30 thermal output power for irradiance 400 W/m$^2$

| **Tm-Ta [C]** | **400 W/m2** |
|---|---|
| 10 | 772 W |
| 30 | 650 W |
| 50 | 490 W |

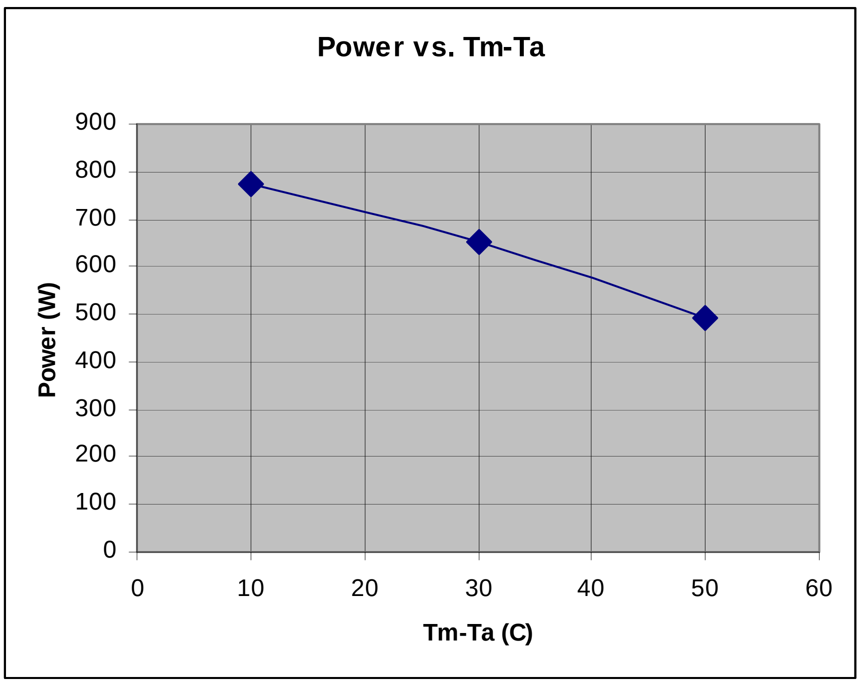


Figure 29: Sunmax-30 thermal output power for irradiance 400 W/m$^2$

Table 4: Evacuated tube design for 400 W/$m^2$

| | |
|---|---|
| Thermal Output Power kW | 16 |
| Gross Area $m^2$ | 155 |
| Aperture Area $m^2$ | 78.1 |
| Number of Evacuated Tubes | 840 |

## 2.4 Conclusions from Theoretical Analysis

Results for irradiance of 1000 W/$m^2$ in Table 2 are obtainable and realistic, where results for irradiance of 400 W/$m^2$ are not realistic as seen in Table 4. For 400 W/$m^2$ conditions, the gross area of the evacuated tubes would not even fit inside the typical foot print of a roof, 90 square meters. Therefore the solar collection system should be designed to produce 16 kW of thermal energy on completely sunny days and not cloudy days. During cloudy days the electrical output will be less than 2 kW. For such days the system should be designed so that the owner can choose to utilize the thermal heat for water heating applications over electrical power production. This will give the consumer the option to benefit from the residential solar power station under all conditions.

During maximum irradiance 2 kW of electricity can be produced. In the summer the peak irradiance lasts for about four hours. This means this design will supply 8 kWh of electricity to consumers. An additional 2 kWh of electricity can be expected for off peak solar hours to result in a maximum of 10 kWh electricity production. This can supplement one third of the average 30 kWh electricity consuming household.

# CHAPTER 3: EXPERIMENTAL DESIGN

## 3.1 Introduction

In theory solar evacuated tubes can reach high enough temperatures and provide enough heat input to drive the residential power system efficiently. But there are many parameters and conditions which will interfere with solar thermal collection. These parameters include the flow rate of the heat transfer liquid, the number of tubes in series, the weather conditions, and the heat losses in the plumbing. To determine an accurate temperature range in which the solar power system can operate, an experiment must be developed to test the amount of heat which can be collected.

## 3.2 Objectives and Operations

$$\dot{Q} = \dot{m} \times C_p \times (T_H - T_C) \qquad (1.2)$$

The experiment will be designed to measure the heat collected from the sun, the high temperatures of the system, and the heat storage capacity of the tank. Equation (1.2) shows that the mass flow rate and change in temperature between the input and the exit of the tubes is a function of heat. The objectives of the experiment are to find the heat collection capacity of the evacuated tubes and from this data, determine how many tubes are necessary to collect 16 kW thermal. The results shall then be compared with the manufacturer's data. The final objective is to gauge how much heat can be extracted from the heat storage tank. This will help determine the design of the expansion device.

The operations of the experiment are defined as actions to measure solar collection components, such as temperature. The most important operation is to measure heat into the system. To measure the collected heat, the change in temperature across the tubes should be measured as well as the flow rate. These values can be inserted into equation (1.2), to find the heat. To gauge how effective the tubes are collecting solar radiation, solar collection efficiency will need to be calculated. To do this the heat collected by the evacuated tubes will be divided by the current radiation from the sun. Therefore an operation to find the current solar radiation will be needed. The high temperature of the system will need to be measured. The highest temperature of the solar collection system will be found at the exit of the last panel of tubes. This temperature will already be measured to find the heat into the system. Another critical temperature is the heat storage tank. It is imperative that the tank maintains high temperatures because this is where the heat of the system will be stored. Temperatures will be measured on the inside of the tank and at the inlet and the exit of the tank. Heat shall be extracted from the tank to resemble the load of the expansion device. This heat extraction will need to be measure, so once again referring to equation (1.2), the change in temperature and flow rate across the storage tank will need to be measured.

Table 5: Experiment Operations

| |
|---|
| Measure change in temperature across the evacuated tubes |
| Measure the flow rate in the solar collection loop |
| Measure the inlet, internal, and exit temperature of the heat storage tank |
| Measure the immediate radiation from the sun |
| Extract heat from the heat storage tank to resemble the expansion device |

## 4.2 Experimental Layout

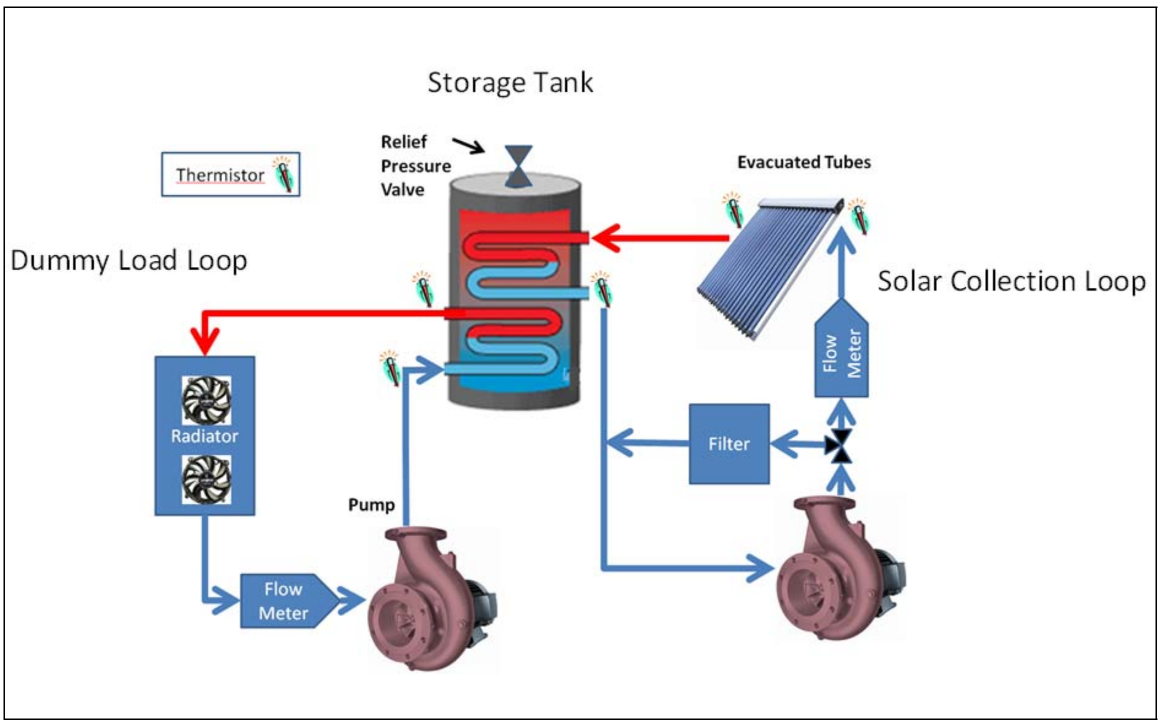


Figure 30: Experimental Layout

The following section will walk through the experimental layout as displayed in Figure 30. The objective of the experiment is to satisfy the operations which need to be performed as defined in Table 5. To determine how much heat the tubes can collect, an array of tubes will be placed in series with thermistors at the inlet and exit of the tubes. The thermistors will measure the temperature at the ends of each panel of tubes. A flow meter will be installed to the plumbing so that the mass flow rate can be determined. A pumped will provide pressure head, driving the heat transfer liquid around the system. The pump will be rated higher than needed. A bypass will be constructed in the plumbing to control the flow rate of the system. The heat collected will be transferred to a heat storage tank. The heat storage tank which acts like a boiler will be connected to a radiator; which will dispel the energy collected. The experiment is to determine the change in temperature across the evacuated tubes at given flow rates, the amount of heat which can be collected, a realistic equilibrium temperature in the heat storage tank, and the effect weather conditions have on the solar collection. In addition different concentrators and reflectors will be utilized around the tubes to determine if they help increase heat collection. A pyranometer will be used to find the available power from the sun in Watts/meter. This measurement can be used to find the efficiency of the system. Water will be used as the heat transfer liquid in this experiment. In the future once the system becomes more refined, an oil will likely be used as a heat transfer liquid so that the experiment can exceed temperatures past 212 °F. (Place an image of experiment overview)

## 3.3 Experimental Instrumentation

Table 6: Required List of Parts

| Hardware | Maker | Model | Quantity |
|---|---|---|---|
| Thermistor | Omega | TH-10-44007 | 8 |
| Flow Meter | Omega | FTB 4605 | 2 |
| Solar Collection Pump | Blue Line Aqua Pump | Blue Line 40 | 1 |
| Radiator Pump | Lang | D5 Solar/710B | 1 |
| Thermal Tank | Sunmaxx | Sunmaxx 150-LSS | 1 |
| Evacuated Tubes | Sunmaxx | Sunmaxx-10 | 2 |
| DAQ | National Instruments | USB 6211 | 1 |

A list of instruments is given in Table 6. For further information regarding the solar tubes, thermistors, and flow meter look to the appendix for manufacturer's information. Figure 31 displays the experimental setup. The number one points to one of the thermistors used to measure the temperature of the fluid. This thermistor is measuring the temperature of the hot fluid coming into the tank from the solar evacuated tubes. The number two corresponds to the flow meter. Three highlights the pump. And four shows the hot water tank, in which the heat is stored. Figure 32 shows the 2, ten evacuated tube panels utilized in the experiment. These instruments were used to measure and analyze the experimental operations and meet the experimental objectives.

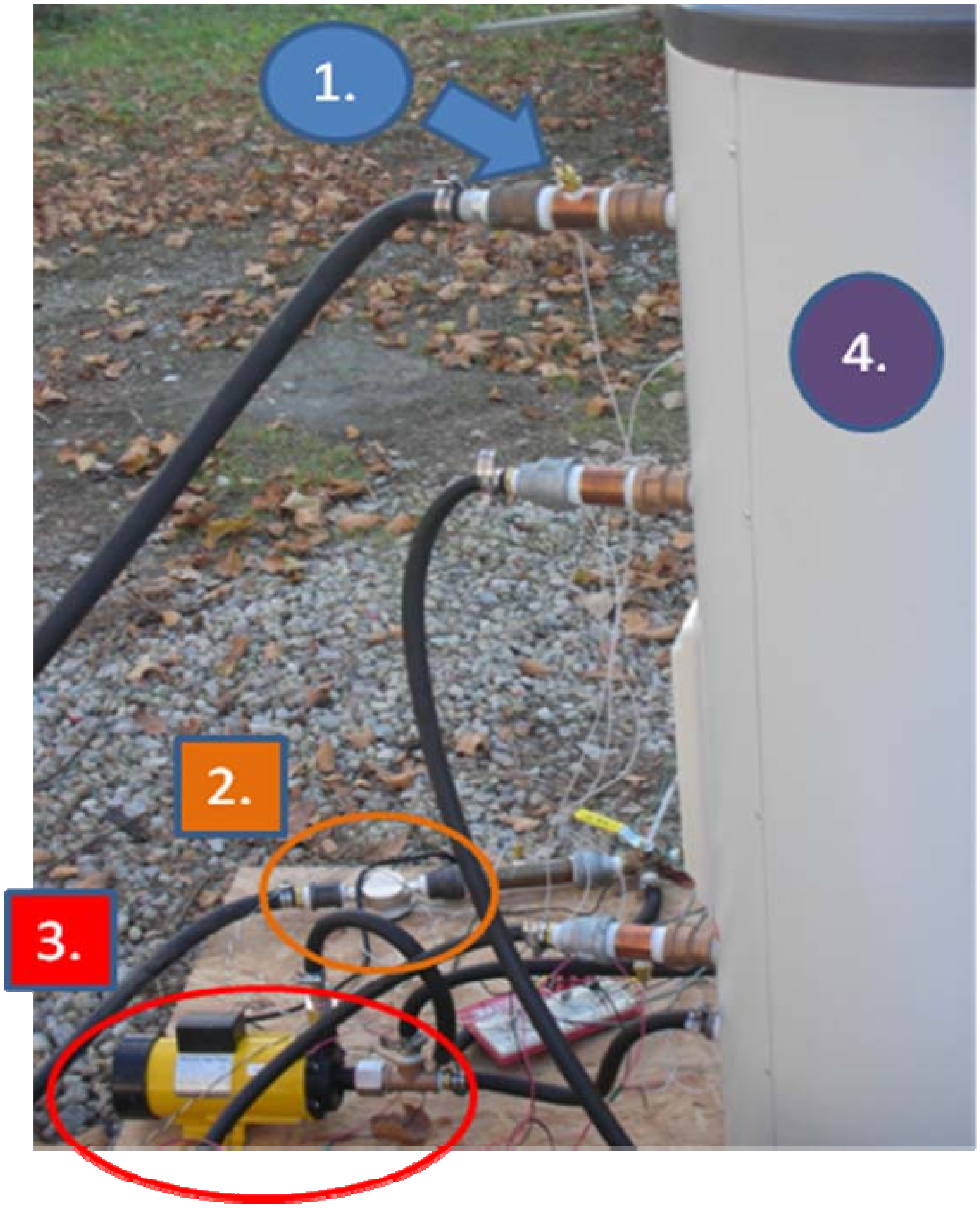


Figure 31: Experimental Instrumentation

Figure 32: Evacuated Tubes with Reflective Aluminum Foil

## 3.4 Experimental Procedure

The experiment shall be constructed per 4.2 Experimental Layout. The experiment will focus solely on the heat collection loop of Figure 30. This means that extracting heat from the heat storage tank to resemble the expansion device will be conducted in the future (Table 5). The panel of tubes shall be constructed and angle the tubes so they face South. Attach a pyranometer to the Sunmaxx Solar manifold so that it sits on a plane parallel to the tubes. Attach thermistors, pyranometer, and flow meter to the data acquisition device. For equations convert pulse reading to data readings refer to the data from the manufacture appendix. Run the experiment with a constant flow rate throughout the day. Place a reflective surface to the backside of the solar tubes as seen in Figure 32. Compare the results between reflective backing and no backing. Perform the experiment operations as defined in Table 5.

# CHAPTER 4: RESULTS AND DISCUSSION

## 4.1 Results for 11/08/10

The following data was taken on the eighth of November 2010 at The Center of Automotive Research in Columbus, Ohio. The mass flow rate through the solar collection loop was 0.34 kg/s. The day was completely sunny with no clouds in the sky. Tests began early in the day shortly after the sun had risen. Figure 33 shows the irradiance of the sun taken from the pyranometer readings. Compare Figure 33 to Figure 24. The graphs are very similar giving confidence the pyranometer is accurately depicting the irradiance of the sun. Figure 33 depicts a perfectly sunny day in November, the best case scenario in the autumn months.

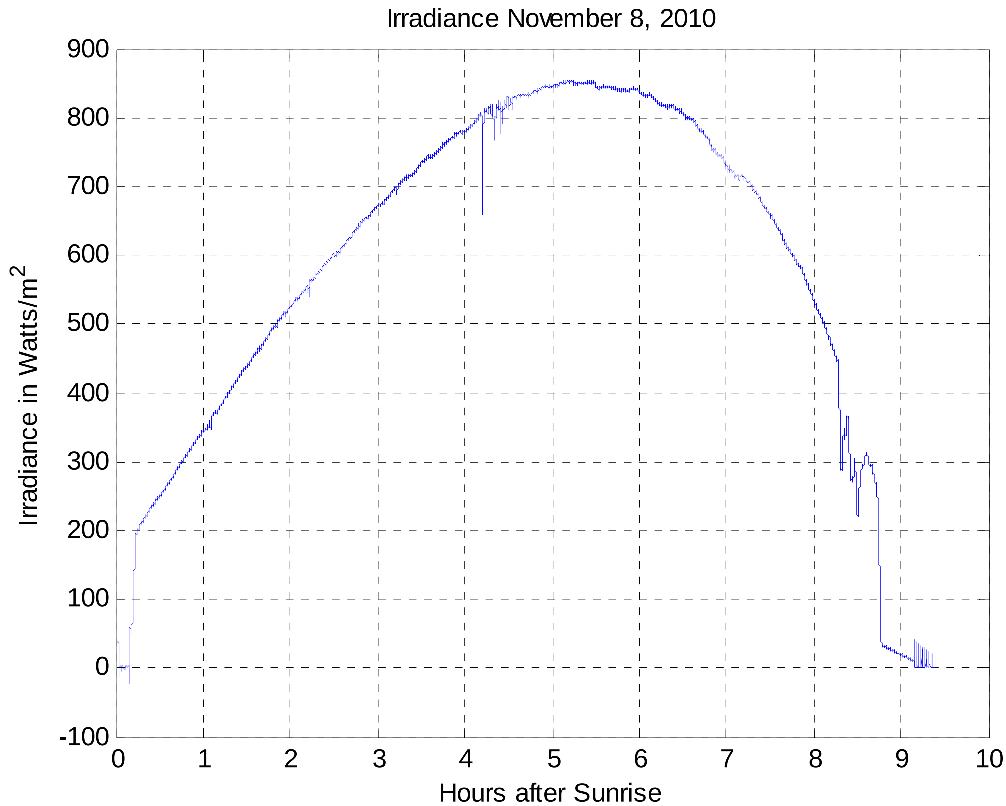


Figure 33: Solar Irradiance for November 8, 2010

Figure 34 displays the temperature increase throughout the day. The thermistor at one of the manifolds was not functioning properly. So the heat in is defined by the change in temperature between the inlet and outlet of the hot water tank. The heat losses can be recognized from the change in temperature between the temperature at the manifold and the inlet of the tank. The water passing through the Sunmaxx Solar Tubes gained only a few degrees in temperature due to the high mass flow rate. The red and green lines are on top of each other suggesting low heat losses. The system is 30 ˚C short of the target temperature of 90 ˚C.

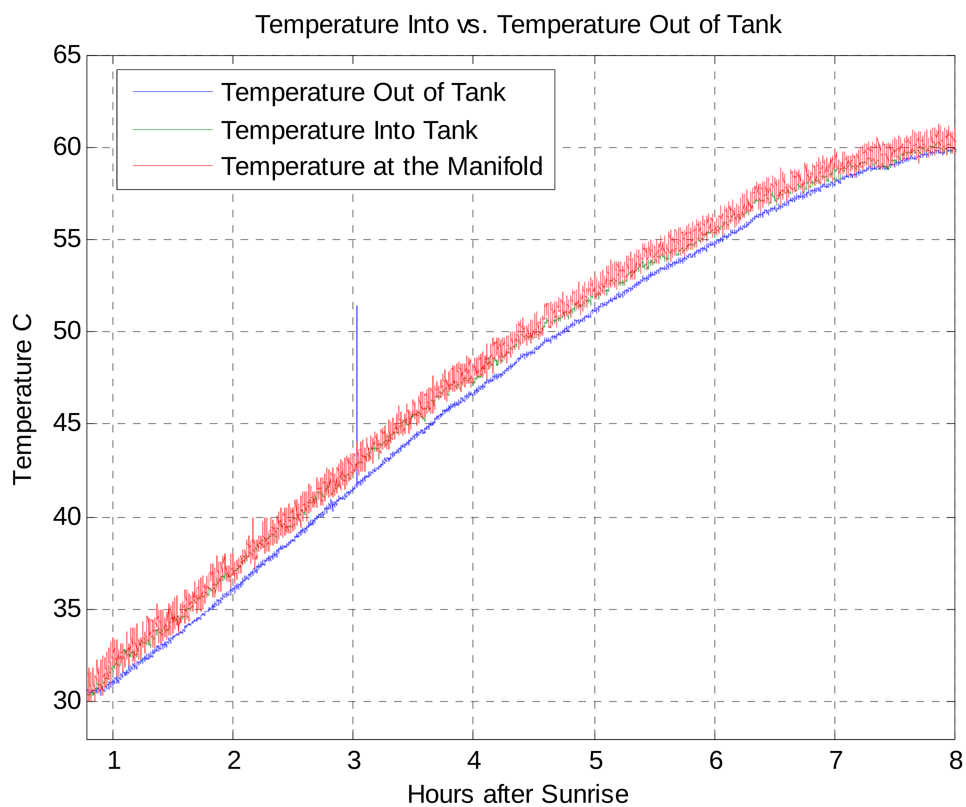


Figure 34: Raw temperature readings throughout the day for increasing temperatures for November 8, 2010

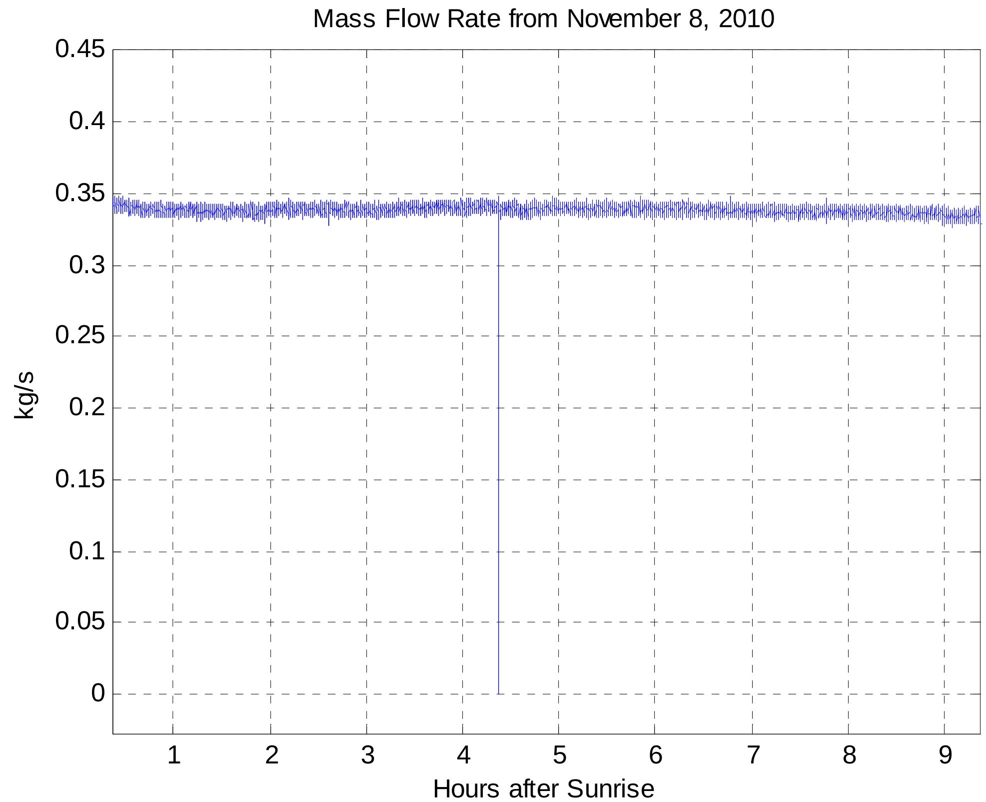


Figure 35: Mass Flow Rate for November 8, 2010

Figure 35 plots the raw data for the measured flow rate. To make the heat captured calculation contain less variability, the flow rate was assumed to be at a constant 0.34 kg/s. This value is taken by observing the flow meter pulsing between values of 0.335 and 0.345 kg/s. At the end of the day the flow meter read values dropping to 0.33 kg/s. Since the experiment is not designed for high accuracy, a constant flow rate of 0.34 kg/s is assumed.

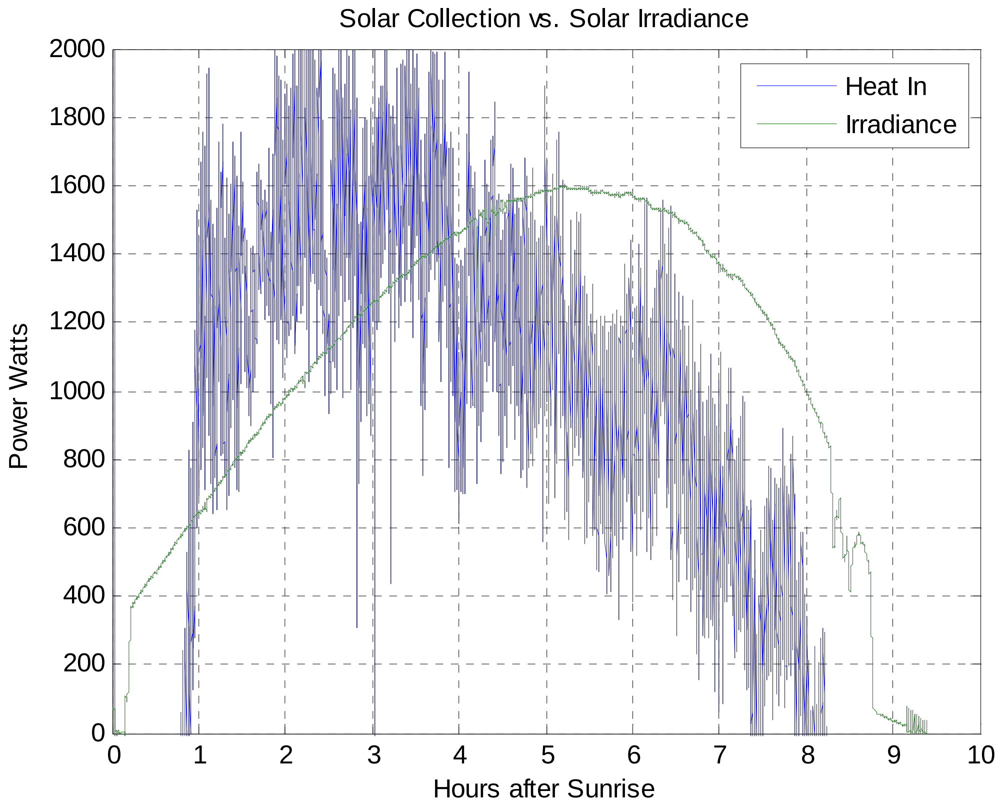


Figure 36: Heat in plotted against Irradiance for November 8, 2010

Using equation (1.2) the heat captured can be calculated. The high temperature is the water coming into the tank and the cold temperature is the water leaving the tank. This temperature difference is shown in Figure 34. The mass flow rate is taken as 0.34 kg/s, as assumed from Figure 35. Figure 36 shows the calculated heat captured compared to the irradiance of the sun using raw data. The heat captured rises above the irradiance which is theoretically not possible. An initial spike above the irradiance is expected because the evacuated tubes were stagnate as the sun was rising. So once flow started travelling through the tubes a spike in temperature ensued. The data suggests that this spiked carried on for hours, which is not true. A source for error in the calculation is that the previous day the water in the tank was heated to test the concept of the experiment. The already hot water may have interfered with the experiment readings. The area under the heat in data and the irradiance data was integrated using the trap function in MATLAB. The heat in was divided by the irradiance to find the solar collection efficiency to be 57%.

## 4.2 Results for 11/09/10

The following data was taken on the ninth of November 2010 at The Center of Automotive Research in Columbus, Ohio. To increase the temperature difference between the outlet and inlet of the tank, the mass flow rate through the solar collection loop was decreased to 0.18 kg/s. Also to improve efficiency the evacuated tubes were given a reflective backing as seen in Figure 32. The day was completely sunny with no clouds in the sky. Tests began late in the morning close to when the sun was peaking. Figure 37 shows the irradiance of the sun taken from the pyranometer readings. Compare Figure 33 to Figure 37. Close to the two hour mark Figure 37 spikes up. This spike may be due to fastening the pyranometer back down on a parallel plane to the tubes. If this were the case from one to two hours the irradiance would be less than expected. The data acquisition somehow became disconnected after hour 5.5 after the test began.

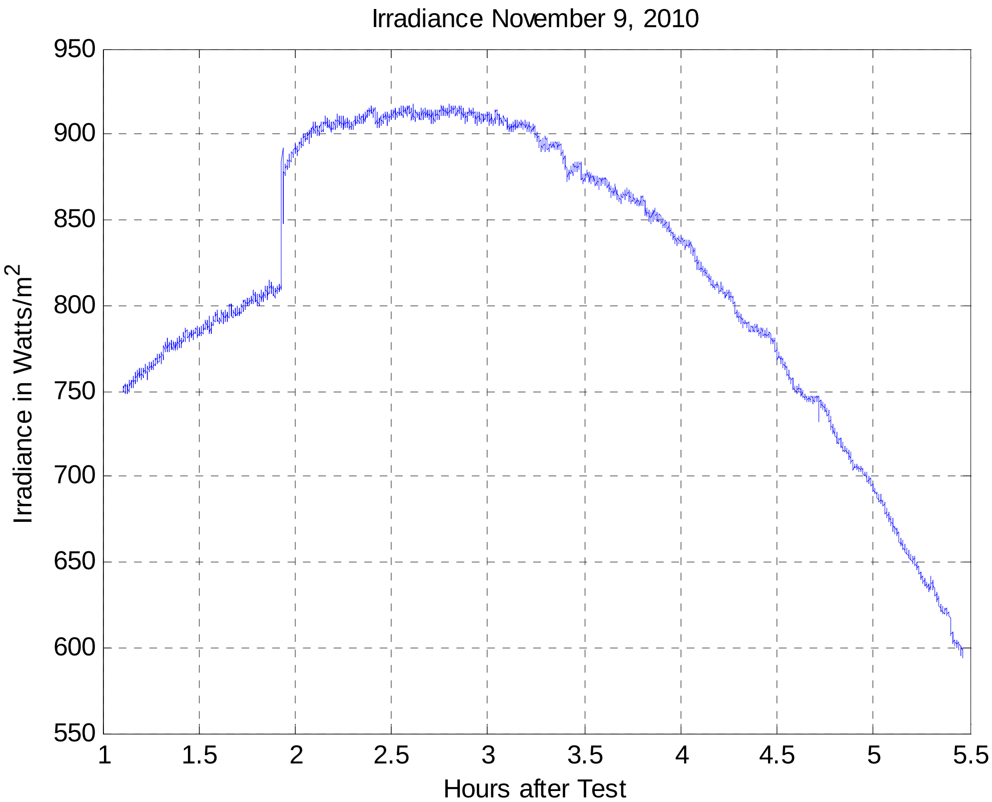


Figure 37: Solar Irradiance for November 9, 2010

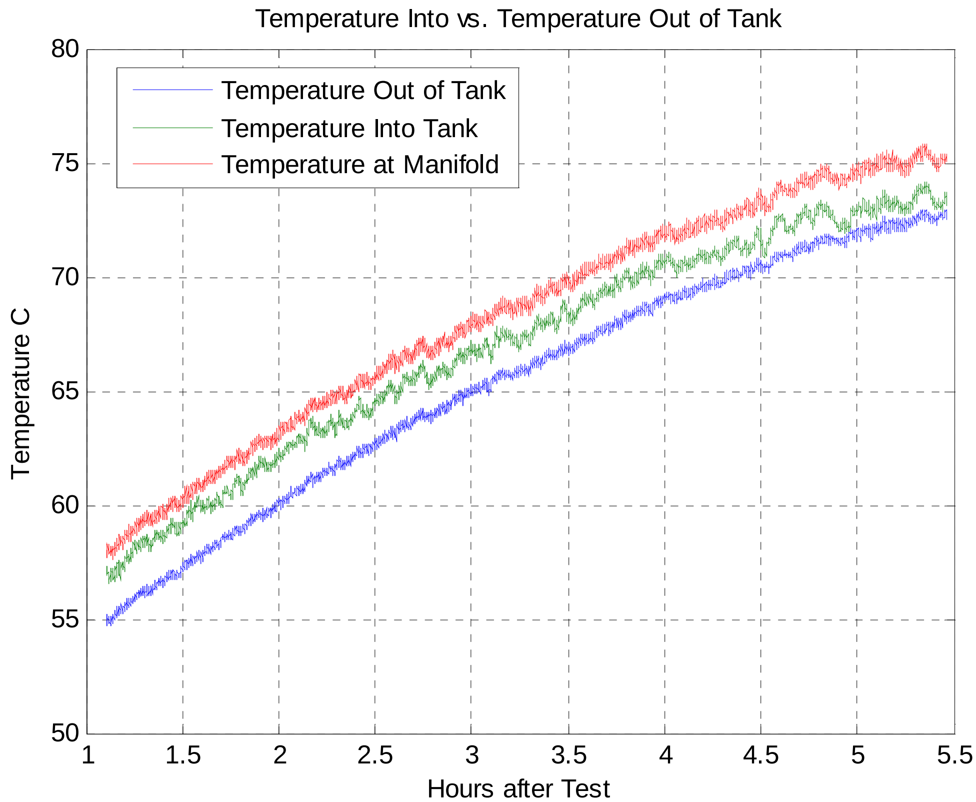


Figure 38: Raw temperature readings throughout the day for increasing temperatures for November 9, 2010

Figure 38 is more pronounced than Figure 34. This is due to the decreased flow rate and reflective background of the tubes. The maximum temperature reached by this system was at the manifold, reaching 75 ˚C. This is 15 ˚C less than the desired temperature needed to drive the Rankine Cycle with Isobutane. The difference between the red and green lines shows the heat lost between the manifold and tank. The heat losses in Figure 38 are more pronounced than in Figure 34. This is once again because the flow rate was nearly halved. Also the system reached higher temperatures, making heat escape at a higher rate to the surrounding conditions. If the piping was properly insulated the tank would be expected to reach higher temperatures.

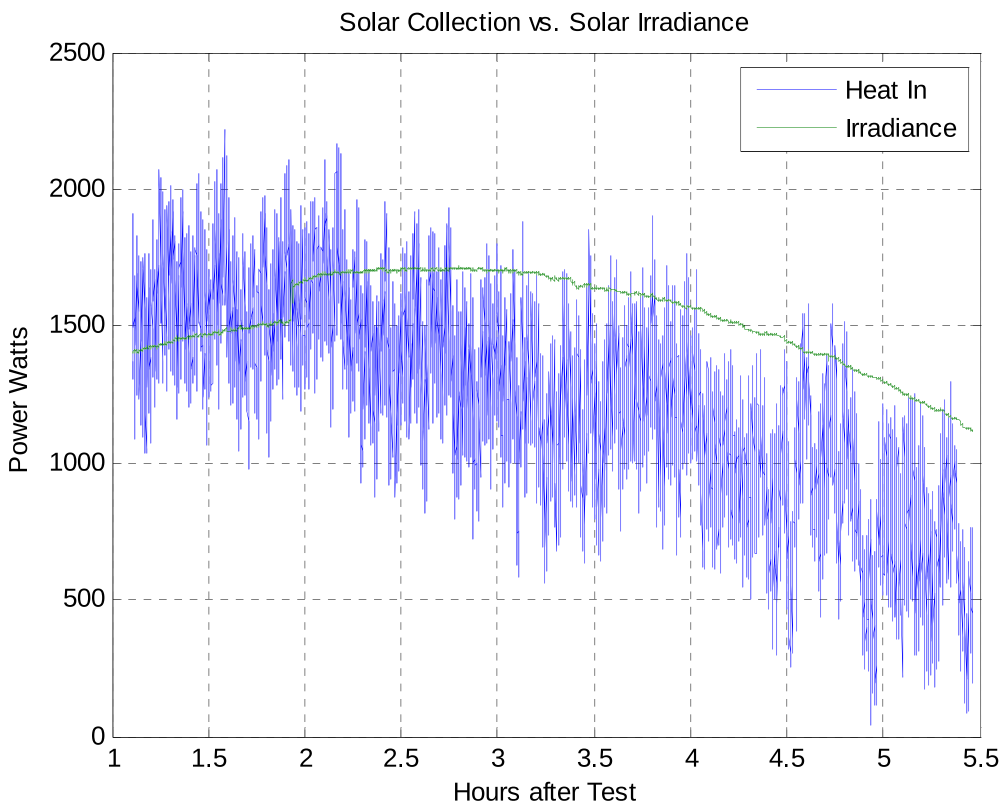


Figure 39: Heat in plotted against Irradiance for November 9, 2010

Figure 39 shows the heat captured versus the irradiance with a reflective background inserted behind the evacuated tubes. The heat captured follows the irradiance very nicely; however, Figure 38 shows that there are noteworthy heat losses in the heat collection system. Figure 37 gives irradiance in Watts per square meters. Notice Figure 39 is in Watts. To get this value the aperture area of the twenty tubes was multiplied by the irradiance to calculate the power available. A reflective background takes the sunshine over a larger area than the aperture area and reflects it to the backside of the tubes. This means there is more power available than Figure 39 suggests. Therefore the efficiency of the solar collection loop of November 9, 2010 as calculated for November 8, 2010 is about 80%. But the actual solar collection efficiency is less than this number because of the extended aperture area due to the reflector. Therefore the heat losses in Figure 38 are possible but do not show in Figure 39.

## 4.3 Results for 11/10/10

The following data was taken on the tenth of November 2010 at The Center of Automotive Research in Columbus, Ohio. The reflective surface was kept as a backing to the tubes and the mass flow rate was kept at 0.16 kg/s. The day was completely sunny with no clouds in the sky. Tests began in the afternoon when the sun had reached its peaking. Figure 40 shows the irradiance of the sun taken from the pyranometer readings. At the end of the day there was some haze moving in resulting in the choppy data in-between hours 4 and 5.

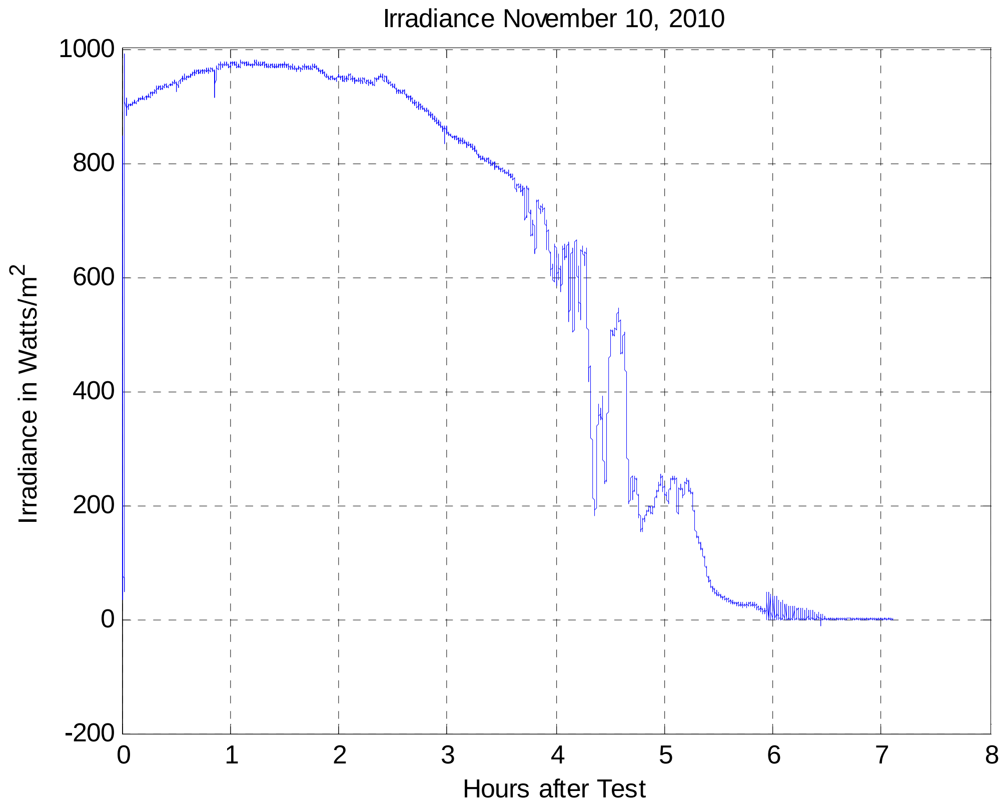


Figure 40: Solar Irradiance for November 10, 2010

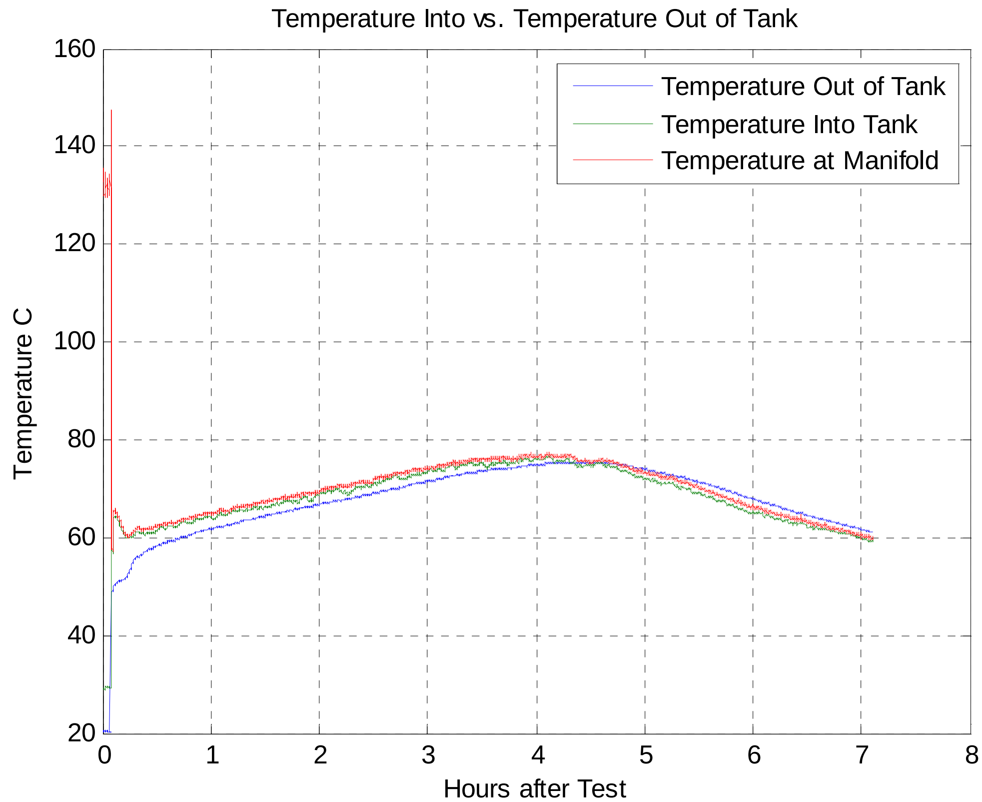


Figure 41: System temperatures for November 10, 2010

The increasing temperature in Figure 41 closely resembles the increasing temperature profile in Figure 38. Figure 41 shows a more complete picture of the test. At the beginning of the test there is a large spike in manifold temperature. The 140 ˚C temperatures are reached at stagnation conditions. This suggests that with more tubes and effective insulation the 90 ˚C target temperature can be obtained. Another interesting point to note is that the system tops out at 75 ˚C again and begins to drop shortly after the fourth hour of testing. Figure 40 shows that the irradiance after the fourth hour of testing is 600 Watts per square meter or less. Therefore the system needs at least 600 Watts per square meter or more irradiance to climb or maintain high temperatures of 75 ˚C. Another method to increase temperature would be to decrease the mass flow rate across the tubes.

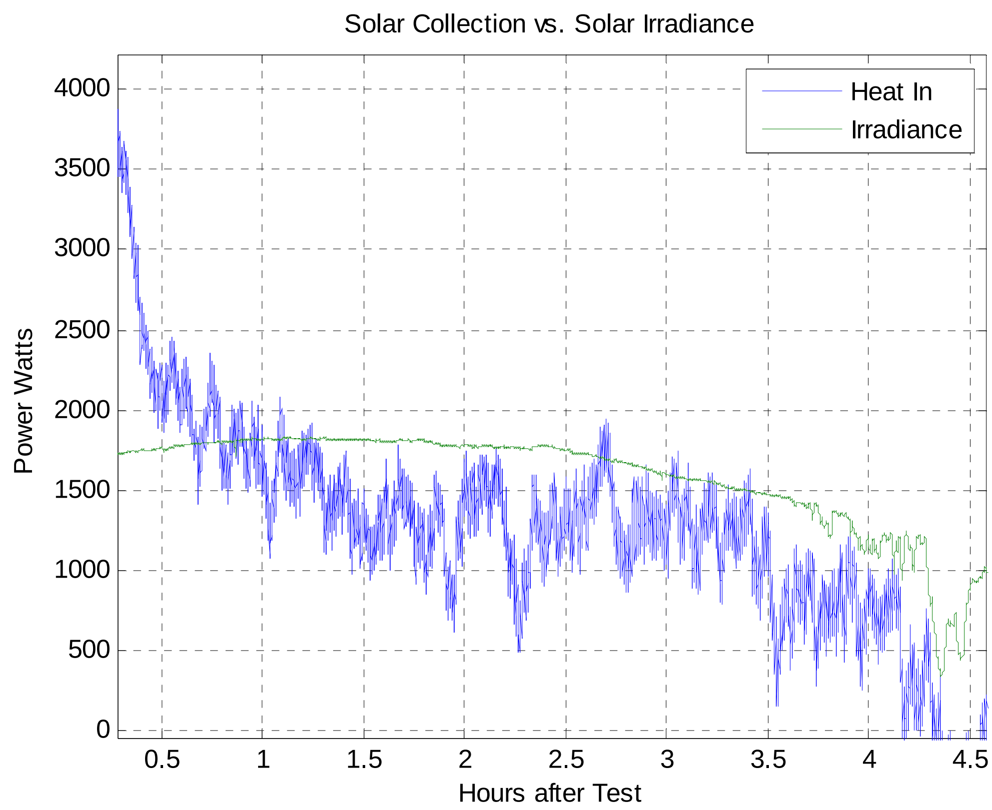


Figure 42: Heat in plotted against Irradiance for November 10, 2010

Figure 42 shows an initial spike in heat collection due to the tubes being at a stagnation state all morning. The graph further confirms the performance of the tubes with the reflector backing. From 0.5 to 4.2 hours of testing the efficiency of the solar collection system was calculated to be 80%, the same as the day previous, under the same conditions.

4.4 Results for 11/15/10

The following data was taken on the fifteenth of November 2010 at The Center of Automotive Research in Columbus, Ohio. The reflective surface was removed and the mass flow rate was kept at 0.18 kg/s. All of the previous data was collected on perfectly sunny days. The results for which were quite favorable. The data collected for this day was not particularly favorable. Figure 43 shows the system only reached 38 ˚C, less than half of the desired temperature. Note the manifold temperature readings seemed inaccurate which is the reason they were excluded from Figure 43. Figure 44 displays the irradiance versus the heat collected which when compared to the other plots shows underperformance. More data should be gathered under poor conditions, but from these initial data points solar heat collection looks bleak for these cloudy conditions.

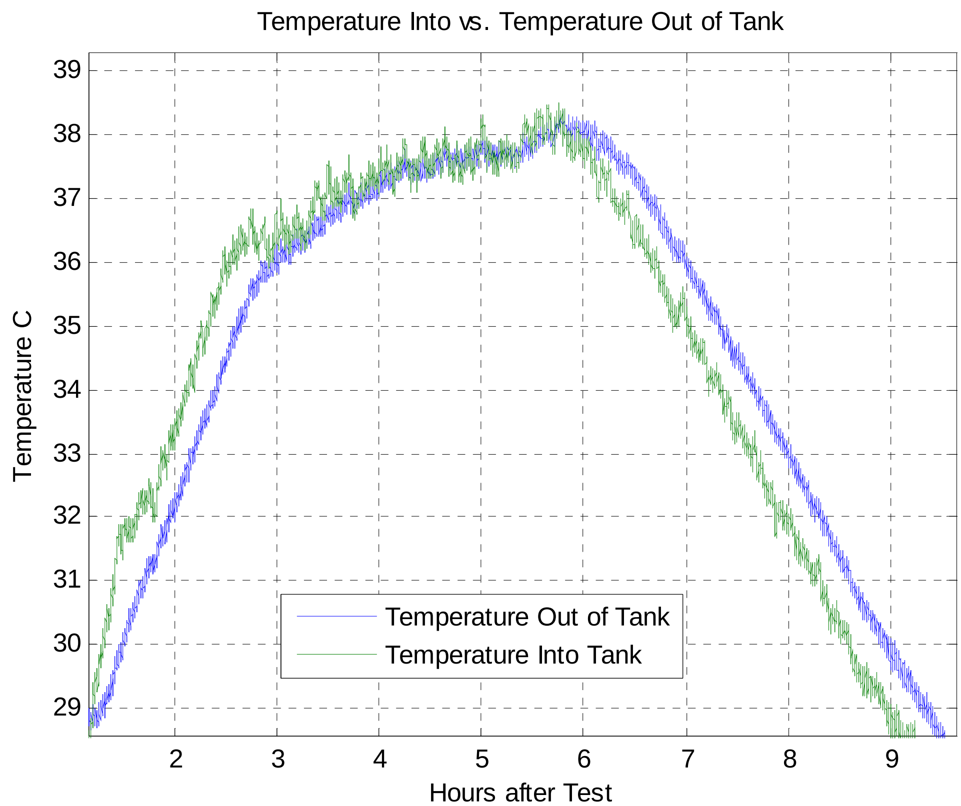


Figure 43: System Temperatures for November 15, 2010

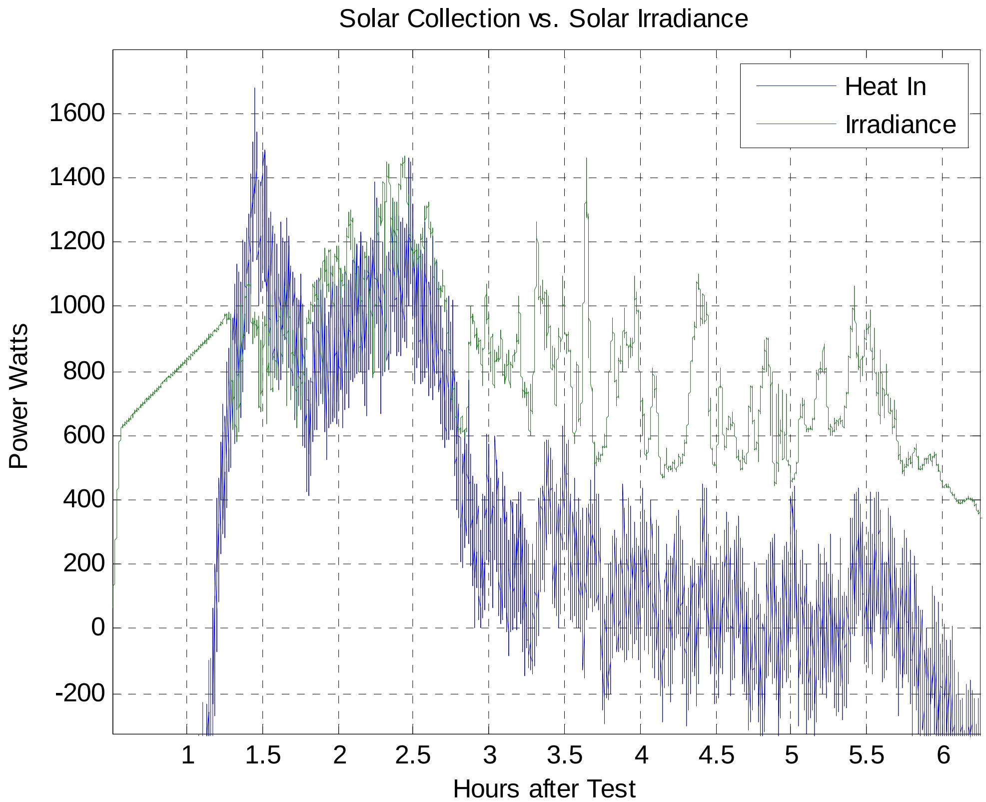


Figure 44: Heat in plotted against Irradiance for November 15, 2010

# CHAPTER 5: CONCLUSION AND RECOMMENDATIONS

## 5.1 Summary

This report investigated the solar thermal collection process to be utilized in a residential Rankine Cycle power plant. The projected rise in fossil fuel prices due to increased emission standards, fossil fuel depletion, and increasing fossil fuel demand gave motivation for designing a new residential solar thermal power plant. Since utility scale solar thermal has been the most cost effective method of solar power production, this report scales the technology down to a residential level. Between parabolic troughs, flat plat solar collectors, and evacuated tubes, the most optimal solar collection tool for residential applications is evacuated tubes. With Isobutane as a working fluid, this report has theoretically shown that under direct sunny conditions a residential system can be designed to produce 10 kWh of electricity. Initial tests show positive results to verify the power production capability, even though the target temperature of 90 ˚C was not reached. The verification tests do not confirm the solar collection system entirely, but gives a positive outlook for future tests and development in the residential solar power plant.

The summary of results can be found in Table 7. When a reflector is added to the system the solar collection performance is enhanced tremendously. Lower flow rates yield higher temperatures, but also yields higher heat losses in the system. The heat losses are not summarized, but can be seen by the change in manifold and inlet tank temperatures in Figure 41. On the best day the system as is missed the target temperature by 15 ˚C. More tests need to be conducted with lower flow rates and better insulation. The initial tests are positive, and with a little refinement the system is projected to operate at the desired conditions.

Table 7: Summary of Results

| Test Date | High Temperature Degrees Celsius | Mass Flow Rate kg/s | Efficiency | Max Irradiance Watts/sqmeter | Reflector |
|---|---|---|---|---|---|
| 11/8/2010 | 60 | 0.34 | 57% | 850 | No |
| 11/9/2010 | 75 | 0.18 | 80% | 930 | Yes |
| 11/10/2010 | 75 | 0.16 | 80% | 990 | Yes |
| 11/15/2010 | 38 | 0.18 | NA | 750 | No |

## 5.2 Recommendations

Evacuated tubes are effective solar collection tools, having the potential to be utilized for residential electrical power applications. While the collection fluid never reached the target temperature, with insulation and an increase in solar tubes, 90 ˚C remains a realistic target for the system to reach. However, if a different Rankine Cycle fluid besides Isobutane is selected operating at high temperatures of 75-80 ˚C, this fluid would be more desirable. The loss in efficiency in the Rankine Cycle from lowering the system high temperature will be made up in the increase in solar collection efficiency.

Placing reflective surfaces to the background of solar tubes makes a large difference in the effectiveness and efficiency of solar collection. With the reflective surface the solar collection efficiency using aperture area jumped from 57% to 80%. The 20% plus jump in efficiency demands that reflective surfaces be utilized in future solar collection designs.

Evacuated tubes were originally picked because they operated in diffused and direct sunlight conditions. With evacuated tubes the solar collection system is being designed for direct sunny conditions due to area constraints. Since parabolic troughs are the best technology for direct sunny conditions, the technology should be investigated to see if the combination of evacuated tubes and parabolic troughs could be utilized to develop an optimal solar thermal collection system for residential power plant applications. Evacuated tubes are effective, but may be more effective if utilized with a parabolic collector.

Insulation will increase the efficiency of the solar collection system. Since the residential solar power plant delivers low power, heat losses are very precious. As the flow rate is further reduced and higher temperatures are reached, higher heat losses are expected. To mitigate these losses and maximize efficiency, sufficient insulation around the piping and copper fixtures shall be installed. This addition should improve solar collection performance.

The current design of 270 evacuated tubes is sufficient to produce 10 kWh of electricity on a sunny summer day. With reflective backgrounds the electricity production may be increased. Continuing to test and refine the solar collection process will yield more efficient methods of collecting thermal energy from the sun. This ground breaking solar collection test is a good first step towards implementing a residential solar thermal power plant.

# WORKS CITED


Cumpsty, N. A. (2009). *Preparing for the Future: Reducing Gas Turbine Enironmental Impact.* Orlando: ASME.

*Department of Energy*. (2010). Retrieved from http://www.eia.doe.gov/oiaf/ieo/highlights.html

*E-solar, Inc.* (2010). Retrieved from http://www.esolar.com/esolar_brochure.pdf

*First Solar, Inc.* (2009). Retrieved from http://firstsolar.com

*Florida State University*. (2010). Retrieved from http://www.eng.fsu.edu

Incropera, F. P. (2007). *Introduction to Heat Transfer.* Hoboken, NJ: John Wiley & Sons.

Korpela, S. (2002). Oil Depletion in the United States and World.

Laherrere, J. (2001). Estimates of Oil Reserves. *EMF/IEA/IEW.* Laxenburg.

Makofske, D. W. (n.d.). Retrieved from Ramapo College of New Jersey: phobos.ramapo.edu/~bmakifsk/energysociety/Photovoltaic%20solar%20Systems.pp

Munsun, B. R. (2009). *Fundementals of Fluid Mechanics.* John Wiley & Sons, Inc.

*National Academy of Engineering*. (2009). Retrieved from http://www.nae.edu

*National Renewable Energy Laboratory*. (2010). Retrieved from http://www.nrel.gov/news/press/2010/889.html

*Northwestern University*. (2010). Retrieved from http://www.qrg.northwestern.edu/thermo/design-library/regen/rnkTs.gif

*NREL*. (2010). Retrieved from http://rredc.nrel.gov/solar/old_data/nsrdb/redbook/atlas/

Quaschning, V. (2010). *Solar Thermal Power Plants*. Retrieved from http://www.volker-quaschning.de/articles/fundamentals2/index.php

Quaschning, V. (2001). *VGB Congress Power Plants 2001*. Brussels.

*Rural Renewable Energy Alliance*. (2008). Retrieved from http://rreal.org/node/51

*Silicon Solar*. (2010). Retrieved from www.siliconsolar.com

*Solar Timeline*. (2010). Retrieved from DOE: (National Renewable Energy Laboratory, 2010)

*The Deparment of Energy*. (2009). Retrieved from http://www.energy.gov

# APPENDIX

Fraunhofer Institut Solare Energiesysteme

Test Report: KTB Nr. 2007-07-ag-k2-en

# Collector test according to EN 12975-1,2:2006

**for:**
SILICON SOLAR INC., USA

**Brand name:**
Sunmaxx-series

**Responsible for testing:**
Dipl.-Ing. (FH) K. Kramer

**Date:**
21st May 2008


**Address:**
Fraunhofer-Institute for Solar Energy Systems ISE
Heidenhofstraße 2, D-79110 Freiburg
Tel.: +49-761-4588-5354; Fax.: +49-761-4588-9354
E-mail: korbinian.kramer@ise.fraunhofer.de
Internet: www.kollektortest.de


Accredited according to DIN EN ISO/IEC 17025:2005

Deutscher Akkreditierungs Rat DAR

ilac-MRA

DIN CERTCO Anerkanntes Prüflaboratorium

Registration No.:
DAP-PL-3926.00

Fraunhofer Institut Solare Energiesysteme

# Contents

# 1 Summary

## 1.1 Preliminary remark

The tests have been performed according to EN 12975-1,2:2006. Main purpose for testing has been, to fulfill all requirements of the SolarKeymark Scheme rules (version 8.0, January 2003).
All requirements have been met.
The certificate of the collector minimum gain of 525 kwh/m$^2$a is handed.

The present report is valid for the Sunmaxx-series including the collectors Sunmaxx-10, Sunmaxx-12, Sunmaxx-14, Sunmaxx-15, Sunmaxx-16, Sunmaxx-18, Sunmaxx-20, Sunmaxx-24, Sunmaxx-25, Sunmaxx-28 and Sunmaxx-30 of the company SILICON SOLAR INC.. The tests were performed at the largest and at the smallest collector of this series.

## 1.2 Collector efficiency parameters determined

Results:
The calculated parameters are based on following areas of the collector Sunmaxx-10 . These parameters are valid for the complete series.

| aperture area of 0.936 m$^2$: | absorber area of 0.808 m$^2$: |
|---|---|
| $\eta_{0a}$ = 0.734 | $\eta_{0A}$ = 0.850 |
| $a_{1a}$ = 1.529 W/m$^2$K | $a_{1A}$ = 1.771 W/m$^2$K |
| $a_{2a}$ = 0.0166 W/m$^2$K$^2$ | $a_{2A}$ = 0.0192 W/m$^2$K$^2$ |

## 1.3 Incidence angle modifier - IAM

| $\theta$: | 0° | 10° | 20° | 30° | 40° | 50° | 53° | 60° | 70° | 80° | 90° |
|---|---|---|---|---|---|---|---|---|---|---|---|
| $K_{\theta T}$: | **1.00** | 1.00 | **1.03** | 1.11 | **1.25** | 1.37 | 1.40 | **1.36** | 1.11 | 0.70 | 0.05 |
| $K_{\theta L}$: | **1.00** | 1.00 | 1.00 | 0.99 | 0.96 | **0.92** | 0.88 | 0.84 | 0.69 | 0.44 | 0.00 |

Table 1: Measured **(bold)** and calculated IAM data for Sunmaxx-10

## 1.4 Effective thermal capacity of the collector

Effective thermal capacity (Sunmaxx-10 ):

14.6 kJ/K

The effective thermal capacity per square meter is (valid for the series):

15.6 kJ/K m$^2$

## 1.5 Schedule of tests and callculations

| Test | Date | Result |
|---|---|---|
| Date of delivery: | October 26th 2006 | |
| 1st internal pressure | November 9th 2006 | passed |
| High temperature resistance | March 3rd 2006 | passed |
| Exposure | October 26th 2006 - 14th March 2007 | passed |
| 1st external thermal shock | November 15th 2006 | passed |
| 2nd external thermal shock | March 8th 2006 | passed |
| 1st internal thermal shock | November 7th 2006 | passed |
| 2nd internal thermal shock | February 15th 2007 | passed |
| Rain penetration | November 15th 2006 | passed |
| Freeze resistance | | not relevant |
| Mechanical load | | passed |
| Stagnation temperature | | 200.3 °C |
| Final inspection | | passed |
| Determination of collector parameters | 13th March 2006 - 15th March 2006 | passed |
| Determination of IAM | | passed |
| Effective thermal capacity | | performed |

## 1.6 Summary statement

No problems or distinctive observations occured during the measurements.

## 2 Test Center

Test Center for Thermal Solar Systems of Fraunhofer ISE
Heidenhofstraße 2, D-79110 Freiburg
Tel.: +49-761-4588-5139 or -5141; Fax.: +49-761-4588-9139
E-mail: korbinian.kramer@ise.fraunhofer.de; rommel@ise.fraunhofer.de
Internet: http://www.kollektortest.de

## 3 Orderer, Expeller, Manufacturer

| | |
|---|---|
| Orderer: | SILICON SOLAR INC.<br>Mr. Adam Farrell<br>Solar Park Bainbridge<br>NY 13733<br>USA<br>Tel: +1-800-653-8540<br>Fax: +1-866-746-5508<br>adam04@siliconsolar.com |
| Expeller: | see orderer |
| Manufacturer: | Jiangsu sunrain solar energy co. ltd<br>Ning hai industrial Zone<br>Lianyungang<br>Tel: 0086 518 8505 180 6<br>Fax: 0086 518 8505 180 8<br>E-mail: jiaoqt@sunrain.com |

# 4 Overview of series Sunmaxx-series collectors

According to the SolarKeymark Scheme rules (version 8.0, January 2003) there is an agreement concerning collectors, wich differ only in size, so called series or families. Only the biggest and the smallest collector have to be tested in this case. A complete collector test according to EN 12975-1,2 has to be performed at the biggest collector. The efficiency test only is sufficient at the smallest collector. The SolarKeymark label based on this tests is valid for the whole series.

(MS) = Manufacturer Specification

| Brand name | test collector | number of tubes | length of tubes |
|---|---|---|---|
| Sunmaxx-10 | yes | 10 | 1.800 m (MS) |
| Sunmaxx-12 | no | 12 (MS) | 1.800 m (MS) |
| Sunmaxx-14 | no | 14 (MS) | 1.800 m (MS) |
| Sunmaxx-15 | no | 15 (MS) | 1.800 m (MS) |
| Sunmaxx-18 | no | 18 (MS) | 1.800 m (MS) |
| Sunmaxx-20 | no | 20 (MS) | 1.800 m (MS) |
| Sunmaxx-24 | no | 24 (MS) | 1.800 m (MS) |
| Sunmaxx-25 | no | 25 (MS) | 1.800 m (MS) |
| Sunmaxx-28 | no | 28 (MS) | 1.800 m (MS) |
| Sunmaxx-30 | yes | 30 | 1.800 m (MS) |

## 4.1 Specific data of the largest collector of the series (Sunmaxx-30 )

| | |
|---|---|
| Brand name: | Sunmaxx-30 |
| Serial no.: | |
| Year of production: | 2006 |
| Number of test collectors: | 1 |
| Collector reference no. (ISE): | 2 KT 57 001 102006 (function tests) |
| Total area: | 2.025 m * 2.420 m = 4.901 $m^2$ |
| Collector depth: | 0.189 m |
| Aperture area: | 1.710 m x 0.0544 m x 30 tubes = 2.791 $m^2$ |
| Absorber area: | 1.710 m x 0.0470 m x 30 tubes = 2.411 $m^2$ |
| Weight empty: | 106 kg |
| Volume of the fluid: | 2,3 l (MS) |

## 4.2 Specific data of the smallest collector of the series (Sunmaxx-10 )

| | |
|---|---|
| Brand name: | Sunmaxx-10 |
| Serial no.: | |
| Year of production: | 2006 |
| Number of test collectors: | 1 |
| Collector reference no.(ISE): | 2 KT 57 003 102006 |
| Total area: | 2.008 m * 0.854 m = 1.715 $m^2$ |
| Collector depth: | 0.189 m |
| Aperture area: | 1.720 m x 0.0544 m x 10 tubes = 0.936 $m^2$ |
| Absorber area: | 1.720 m x 0.0470 m x 10 tubes = 0.808 $m^2$ |
| Weight empty: | 39.6 kg |
| Volume of the fluid: | 0,7 l (MS) |

## 4.3 Specification of the tubes

(MS) = Manufacturer Specification

| | |
|---|---|
| Type: | vacuum tube collector<br>heat pipe, dry conection<br>without mirror |
| Material of the cover tube: | borosilicate glass (MS) |
| Transmission of the cover tube: | $\geq$ 91 % (MS) |
| Outer diameter of the cover tube: | 0.058 m (MS) |
| Thickness of the cover tube: | 0.0018 m (MS) |
| Outer diameter of the inner tube | 0.047 m (MS) |
| Thickness of the inner tube: | 0.0016 m (MS) |
| Distance from tube to tube: | 0.078 m (MS) |

### 4.4 Absorber

| | |
|---|---|
| Material of the absorber: | Cu/Al/SS/$N_2$ on borosilicate glass (MS) |
| Kind/Brand of selective coating: | ALN/SS-ALN/Cu (MS) |
| Absorptivity coefficient $\alpha$: | $\geq$ 94 % (MS) |
| Emissivity coefficient $\varepsilon$: | $\leq$ 7 % (MS) |
| Material of the absorber pipes: | copper (MS) |
| Layout of the absorber pipes: | heat pipe, dry conection (MS) |
| Outer diameter: | 0.008 m (MS) |
| Inner diameter: | 0.0068 m (MS) |
| Material of the header pipe: | copper (MS) |
| Outer diameter of the header pipe: | 0.038 m (MS) |
| Inner diameter of the header pipe: | 0.034 m (MS) |
| Material of the contact sheets: | aluminium (MS) |
| Thickness of the contact sheets: | 0.0002 m (MS) |

### 4.5 Insulation and Casing

| | |
|---|---|
| Medium between the inner and outer tubes of the vacuum flask: | high vacuum (MS) |
| Thickness of the insulation in the header: | 0.040 m (MS) |
| Material: | polyurethane, mineral wool (MS) |
| Material of the casing: | aluminium (MS) |
| Sealing material: | silicon rubber (MS) |

### 4.6 Limitations

| | |
|---|---|
| Maximum fluid pressure: | 1000 kPa (MS) |
| Operating fluid pressure: | 600 kPa (MS) |
| Maximum service temperature: | 95 °C (MS) |
| Maximum stagnation temperature: | 200.3 °C |
| Maximum wind load: | not spezified |
| Recommended tilt angle: | 15 °- 75 °(MS) |
| Flow range recommendation: | 50 -150 l/m$^2$h (MS) |

## 4.7 Kind of mounting

| | |
|---|---|
| Flat roof - mounted on the roof: | yes (MS) |
| Tilted roof - mounted on the roof: | no (MS) |
| Tilted roof - integrated: | yes (MS) |
| Free mounting: | no (MS) |
| Fassade: | yes (MS) |

## 4.8 Picture and cut drawing of the collector

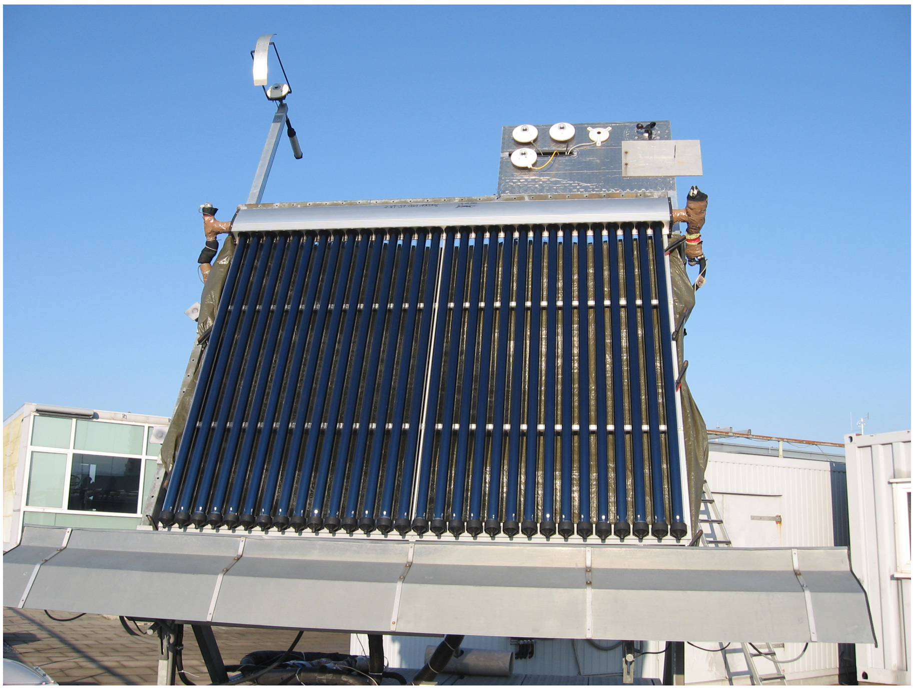

Figure 1: Picture of the collector Sunmaxx-30 mounted on the test facility of Fraunhofer ISE

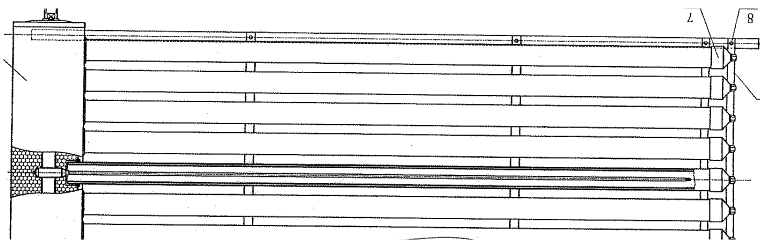

Figure 2: Cut drawing of the collector Sunmaxx-10

# 5 Collector efficiency parameters

## 5.1 Test method

Outdoor, steady state according to EN 12975-2:2006 (tracker)
Thermal solar systems and components - solar collectors,
Part 2: Test methods

## 5.2 Description of the calculation

The functional dependence of the collector efficiency on the meteorological and system operation values can be represented by the following mathematical equation:

$$\eta_{(G,(t_m - t_a))} = \eta_0 - a_{1a}\frac{t_m - t_a}{G} - a_{2a}\frac{(t_m - t_a)^2}{G} \quad (1)$$

(based on aperture area)

$$t_m = \frac{t_e + t_{in}}{2}$$

where:
$G$ = global irradiance on the collector area (W/m$^2$)
$t_{in}$ = collector inlet temperature (°C)
$t_e$ = collector outlet temperture (°C)
$t_a$ = ambient temperature (°C)

The coefficients $\eta_0$, $a_{1a}$ and $a_{2a}$ have the following meaning:

$\eta_0$: Efficiency without heat losses, which means that the mean collector fluid temperature is equal to the ambient temperature:

$$t_m = t_a$$

The coefficients $a_{1a}$ and $a_{2a}$ describe the heat loss of the collector. The temperature depedency of the collector heat loss is described by:

$$a_{1a} + a_{2a} * (t_m - t_a)$$

## 5.3 Efficiency parameters

Boundary conditions:

As the collector is constructed without a reflector or another defined reflecting backside, the effincy messurements were performed by using a tarpaulin with a defined absorption coefficient of 83 %. This corresponds to typical absorption coefficients of common rooftile.

| | |
|---|---|
| Test method: | outdoor, steady state |
| Latitude: | 48.0° |
| Longitude: | 7.8° |
| Collector tilt: | tracked between 35°and 55° |
| Collector azimuth: | tracked |
| Mean irradiation : | 936 $W/m^2$ |
| Mean wind speed: | 3 m/s |
| Mean flow rate: | 66 kg/h |
| Kind of fluid: | water |
| date of the Measurement | February 2007 |

Results:
The calculated parameters are based on following areas of the collector Sunmaxx-10 . These values are also valid for the complete series.[1]:

| aperture area of 0.936 $m^2$: | absorber area of 0.808 $m^2$: |
|---|---|
| $\eta_{0a}$ = 0.734 | $\eta_{0A}$ = 0.850 |
| $a_{1a}$ = 1.529 $W/m^2K$ | $a_{1A}$ = 1.771 $W/m^2K$ |
| $a_{2a}$ = 0.0166 $W/m^2K^2$ | $a_{2A}$ = 0.0192 $W/m^2K^2$ |

The determination for the standard deviation (k=2) was performed according ENV 13025 (GUM). Based on this calculation the uncertainty is less than 2%-points of the efficiency values over the complete measured temperature range ( $\eta_{0a}$ = 0.734 +/- 0.02). Based on our experience with the test facilities the uncertainty is much smaller and in a range of **+/- 1%-point**. The standard deviation of the heat loss parameters resulting from the regression fit curve through the measurement points is: $a_{1a}$ = 1.529 +/- 0.0686 and $a_{2a}$ = 0.0166 +/- 0.0008 .

For more detailed data and the calculated efficiency curve please see annex B.

[1] absorber area - projected area of absorber tube,
aperture area - projected area of inner diameter of cover tube

## 5.4 Power output per collector unit

The power output per collector unit will be documented for the largest collector of the series Sunmaxx-30 with the highest output per collector unit and for the smallest collector of the series Sunmaxx-10 with the lowest output per collector unit.

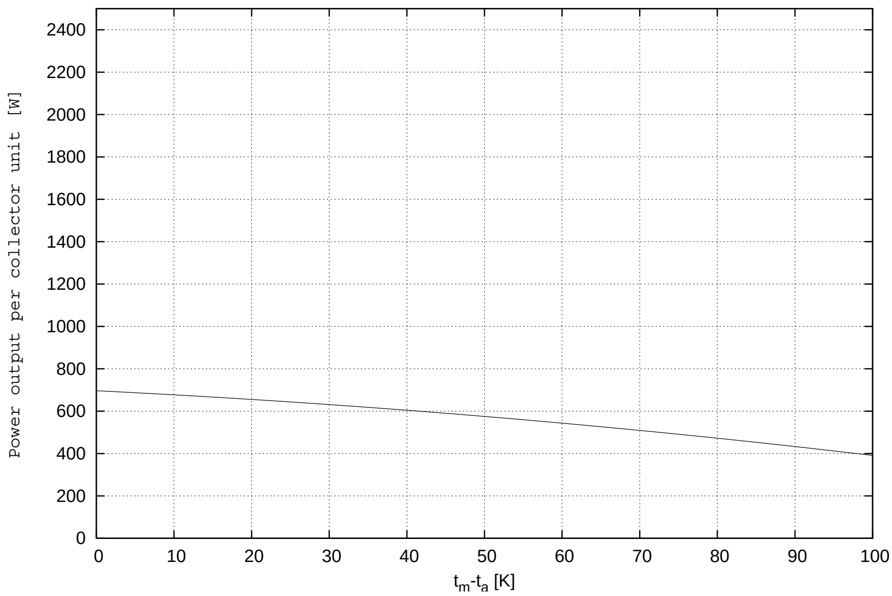


Figure 3: Power output for collector Sunmaxx-10 based on 1000 W/m$^2$

Power output per collector unit [W] for collector Sunmaxx-10 (aperture area of 0.936 m$^2$):

| $t_m - t_a$ [K] | 400 [W/m$^2$] | 700 [W/m$^2$] | 1000 [W/m$^2$] |
|---|---|---|---|
| 10 | 259 | 465 | 671 |
| 30 | 218 | 424 | 630 |
| 50 | 164 | 371 | 577 |

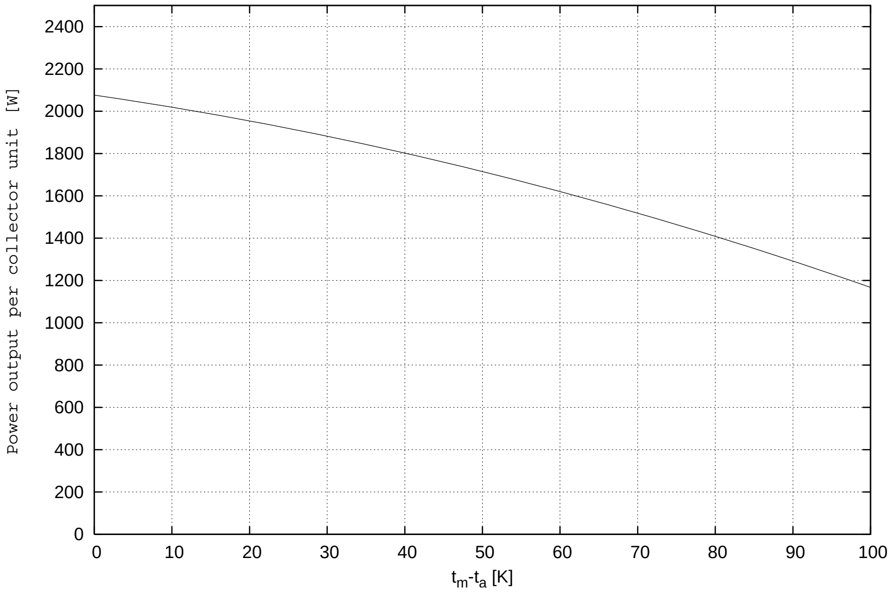


Figure 4: Power output for collector Sunmaxx-30 based on 1000 W/m²

Power output per collector unit [W] for collector Sunmaxx-30 (aperture area of 2.791 m²):

| $t_m - t_a$ [K] | 400 [W/m²] | 700 [W/m²] | 1000 [W/m²] |
|---|---|---|---|
| 10 | 772 | 1387 | 2001 |
| 30 | 650 | 1264 | 1879 |
| 50 | 490 | 1105 | 1719 |

The power output per collector unit can be calculated for other collectors of this series according to the follwoing procedure:

$$P = P_{ref} * \frac{A_a}{A_{a,ref}}$$

with:

| | |
|---|---|
| $P$ | = Collector output for a different collector of the series |
| $P_{ref}$ | = Collector output for collector Sunmaxx-10 , (values see table) |
| $A_a$ | = Aperture area of a different collector of the series |
| $A_{a,ref}$ | = Aperture area of collector Sunmaxx-10 = 0.936 m² |

## 6 Incidence angle modifier IAM

The IAM (= Incidence Angle Modifier) is a correction factor representing how the angle of incident radiation affects the performance of a collector. For collectors which have a direction-depending IAM behaviour (for example vacuum tube collectors and collectors with CPC reflectors), it is necessary to meassure the IAM for more than one direction, to have a proper determination of the IAM.

The complex IAM can be estimated by calculating it as the product of both separately meassured incidence angle modifiers $K_{\theta L}$ and $K_{\theta T}$ of two orthogonal planes (equation 2).

$$K_\theta = K_{\theta L} x K_{\theta T} \quad (2)$$

The longitudinal plane (index L) is orientated parallelly to the optical axsis of the collector. The transversal plane is orientated orthogonally to the optical axsis of the collector. The angles $\theta T$ and $\theta L$ are the projection of the incidance angle of the radiation on the transversal or longitudinal plane.

| | |
|---|---|
| Test method: | outdoor, steady state |
| Latitude: | 48.0° |
| Longitude: | 7.8° |
| Collector tilt: | tracked |
| Collector azimuth: | tracked |

| $\theta$: | 0° | 10° | 20° | 30° | 40° | 50° | 53° | 60° | 70° | 80° | 90° |
|---|---|---|---|---|---|---|---|---|---|---|---|
| $K_{\theta T}$: | **1.00** | 1.00 | **1.03** | 1.11 | **1.25** | 1.37 | 1.40 | **1.36** | 1.11 | 0.70 | 0.05 |
| $K_{\theta L}$: | **1.00** | 1.00 | 1.00 | 0.99 | 0.96 | **0.92** | 0.88 | 0.84 | 0.69 | 0.44 | 0.00 |

Table 2: Measured **(bold)** and calculated IAM data for Sunmaxx-10

The angles for the transversal IAM in table 2 were calculated according to Ambrosetti [1](equation 3).

$$K_\theta = 1 - [tan\frac{\theta}{2}]^{\frac{1}{r}} \quad (3)$$

[1] P.Ambrosetti. Das neue Bruttowärmeertragsmodell für verglaste Sonnenkollektoren, Teil 1 Grundlagen. EIR, Wurenlingen 1983

# 7 Effective thermal capacity of the collector

The effective thermal capacity of the collector is calculated according to section 6.1.6.2 of EN 12975-2:2006. For the heat transfer fluid a mixture 2/1 of water/propylenglycol at a temperature of 50°C has been chosen.

Effective thermal capacity (Sunmaxx-10 ):

14.6 kJ/K

The effective thermal capacity per square meter is (valid for the series):

15.6 kJ/K $m^2$

# 8 Internal pressure test

| | |
|---|---|
| Maximum pressure: | 1000 kPa (MS) |
| Test temperature: | 12.3 °C |
| Test pressure: | 1500 kPa (1.5 times the maximum pressure) |
| Test duration: | 15 min |

Result:
During and after the test no leakage, swelling or distortion was observed or measured.

# 9 High temperature resistance test

| Method: | Indoor testing |
|---|---|
| Collector tilt angle: | 45° |
| Average irradiance during test: | 1011 $W/m^2$ |
| Average surrounding air temperature: | 25.3 °C |
| Average surrounding air speed: | < 0.5 m/s |
| Average absorber temperature: | 197,5 °C |
| Duration of test: | 1 h |

Result:
No degradation, distortion, shrinkage or outgassing was observed or measured at the collector.

## 10 Exposure test

The collector tilt angle was 45° facing south. Annex C shows all test days of the exposure test.

Result:
The number of days when the daily global irradiance was more than 14 MJ/m$^2$d was 41 . The periods when the global irradiance $G$ was higher than 850 W/m$^2$ and the surrounding air temperature $t_a$ was higher than 10 °C was 41.7 h.

The evaluation of the exposure test is described in the chapter 17 "Final inspection".

## 11 External thermal shock tests

| Test conditions | 1st test | 2nd test |
|---|---|---|
| Outdoors: | yes | yes |
| Combined with exposure test: | yes | yes |
| Combined with high temperatur resistance test: | no | no |
| Collector tilt angle: | 45° | 45° |
| Average irradiance: | 850 W/m$^2$ | 860 W/m$^2$ |
| Average surrounding air temperature: | 17.8 °C | 12.6°C |
| Period during which the required operating conditions were maintained prior to external thermal shock: | 1 h | 1 h |
| Flowrate of water spray: | 0.05 l/m$^2$ s | 0.05 l/m$^2$ s |
| Temperature of water spray: | 16.6 °C | 16.0 °C |
| Duration of water spray: | 15 min | 15 min |
| Absorber temperature immediately prior to water spray: | 162.0 °C | 159.1°C |

Result:
No cracking, distortion, condensation or water penetration was observed or measured at the collector.

# 12 Internal thermal shock tests

| Test conditions | 1st test | 2nd test |
|---|---|---|
| Outdoors: | yes | yes |
| Combined with exposure test: | yes | yes |
| Combined with high temperature resistance test: | no | no |
| Collector tilt angle: | 45° | 45° |
| Average irradiance: | 884 W/m$^2$ | 957 W/m$^2$ |
| Average surrounding air temperature: | 9.8 °C | 10.4 °C |
| Period during which the required operating conditions were maintained prior to internal thermal shock: | 1 h | 1 h |
| Flowrate of heat transfer fluid: | 0.02 l/m$^2$ s | 0.02 l/m$^2$ s |
| Temperature of heat transfer fluid: | 16.6 °C | 16.4 °C |
| Duration of heat transfer fluid flow: | 5 min | 5 min |
| Absorber temperature immediately prior to heat transfer fluid flow: | 160.0 °C | 180.2 °C |

No cracking, distortion or condensation was observed or measured at the collector.

# 13 Rain penetration test

| | |
|---|---|
| Collector mounted on: | Open frame |
| Method to keep the absorber warm: | Exposure of collector to solar radiation |
| Flowrate of water spray: | 0.05 l/m$^2$ s |
| Duration of water spray: | 4 h |

Result:
No water penetration was observed or measured at the collector.

# 14 Freeze resistance test

The freeze resistance test is not relevant, because the manufacturer suggestst a application of the collector only with a freeze resistance fluid.

# 15 Mechanical load test

## 15.1 Positive pressure test of the collector cover

This test was not performed by means of implementing pressure. The collector was visualy observed and the structur was checked from a technical point of view.

### 15.2 Negative pressure test of fixings between the cover and the collector box

This test was not performed by means of implementing pressure. The collector was visualy observed and the structur was checked from a technical point of view.

### 15.3 Negative pressure test of mountings

The mechanical load test is not reasonable for this collector because of the vacuum tube type without reflector.

## 16 Stagnation temperature

The stagnation temperature was measured outdoors. The measured data are shown in the table below. To determine the stagnation temperature, these data were extrapolated to an irradiance of 1000 W/m$^2$ and an ambient temperatur of 30 °C. The calculation is as follows:

$$t_{\mathrm{s}} = t_{\mathrm{as}} + \frac{G_{\mathrm{s}}}{G_{\mathrm{m}}} * (t_{\mathrm{sm}} - t_{\mathrm{am}}) \quad (4)$$

$t_{\mathrm{s}}$: Stagnation temperature
$t_{\mathrm{as}}$: 30 °C
$G_{\mathrm{s}}$: 1000 W/m$^2$
$G_{\mathrm{m}}$: Solar irradiance on collector plane
$t_{\mathrm{sm}}$: Absorber temperature
$t_{\mathrm{am}}$: Surrounding air temperature

| Irradiance | Surrounding air temperature | Absorber temperature |
|---|---|---|
| [W/m$^2$] | [°C] | [°C] |
| 1008 | 13.1 | 182.8 |
| 994 | 13.5 | 181.7 |
| 967 | 13.8 | 179.2 |
| 948 | 13.8 | 174.7 |
| 988 | 12.4 | 183.3 |

The resulting stagnation temperature is:

200.3 °C

## 17 Final inspection

The following table shows an overview of the result of the final inspection.

| Collector component | Potential problem | Evaluation |
|---|---|---|
| Collector box/ fasteners | Cracking/ wraping/ corrosion/ rain penetration | 0 |
| Mountings/ structure | Strength/ safety | 0 |
| Seals/ gaskets | Cracking/ adhesion/ elasticity | 0 |
| Cover/ reflector | Cracking/ crazing/ buckling/ delamination/ wraping/ outgassing | 0 |
| Absorber coating | Cracking/ crazing/ blistering | 0 |
| Absorber tubes and headers | Deformation/ corrosion/ leakage/ loss of bonding | 0 |
| Absorber mountings | Deformation/ corrosion | 0 |
| Insulation | Water retention/ outgassing/ degradation | 0 |

0: No problem
1: Minor problem
2: Severe problem
x: Inspection to establish the condition was not possible

## 18 Collector identification

The collector identification/documentation according EN 12975-1 chapter 7 was complete, see the following items:

- Drawings and data sheet
- Labeling of the collector
- Installer instruction manual
  (not for mounting integrated in tilted roof or fassade mounting, no pressure lost)
- List of used materials

## 19 Summary statement

The measurements were carried out from
October 2006 until February 2007 .

No problems or distinctive observations occured during the measurements.

## 20 Annotation to the test report

The results described in this test report refer only to the test collector. It is not allowed to make extract copies of this test report.

Test report: KTB Nr. 2007-07-ag-k2-en

Freiburg, 21st May 2008
Fraunhofer-Institute for Solar Energy Systems ISE

| | |
|---|---|
| Dipl.-Phys. M. Rommel<br>Head of the Test Center for<br>Thermal Solar Systems | Dipl.-Ing. (FH) K. Kramer<br>Responsible for testing<br>and report |

# A Drawing of absorber layout

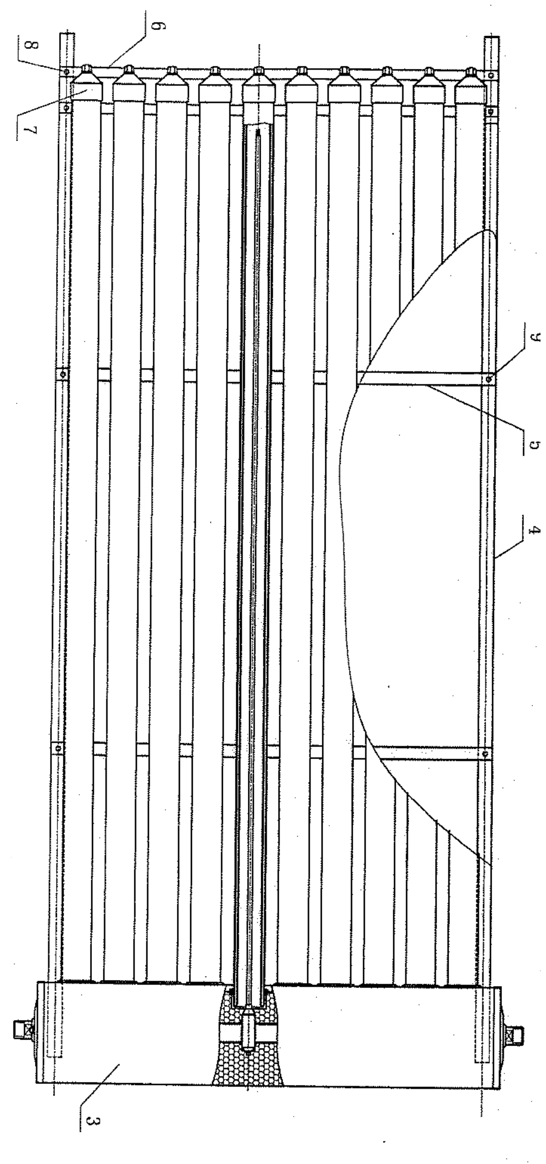


Figure 5: Drawing of absorber layout Sunmaxx-10

# B Efficiency curve

## B.1 Efficiency curve with measurement points based on aperture area 0.936 $m^2$

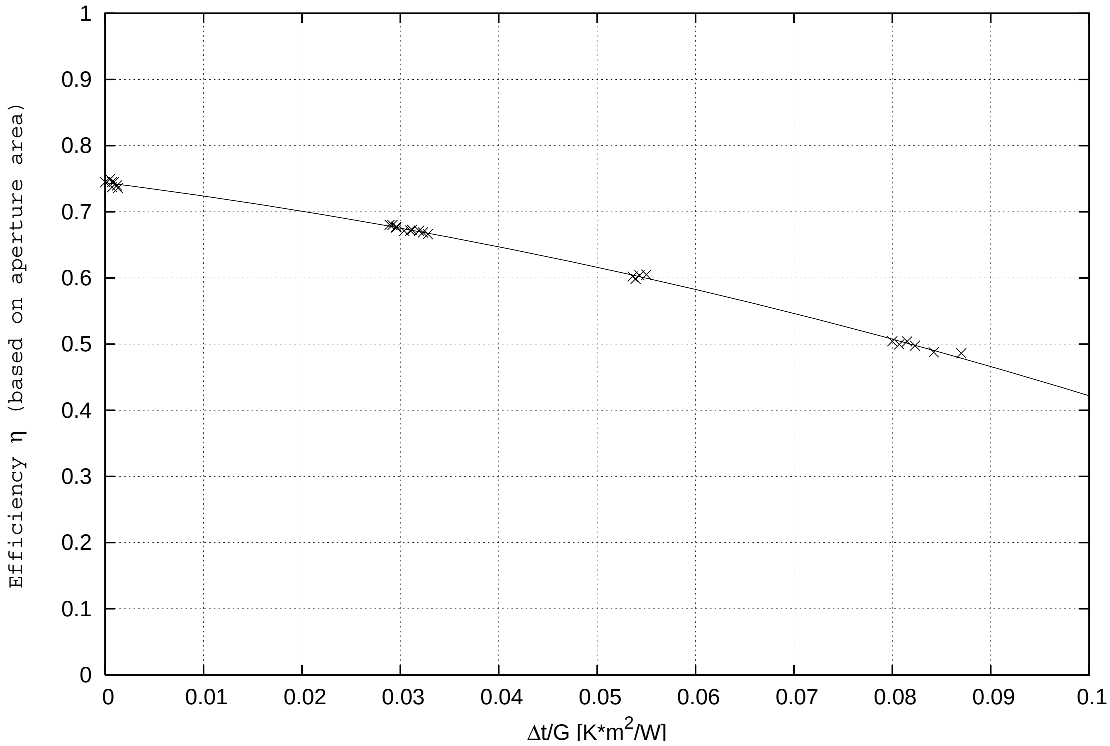


Figure 6: Efficiency curve with measurement points based on aperture area 0.936 $m^2$

Results:

The calculated parameters are based on following areas:

| aperture area of 0.936 $m^2$: | absorber area of 0.808 $m^2$: |
|---|---|
| $\eta_{0a}$ = 0.734 | $\eta_{0A}$ = 0.850 |
| $a_{1a}$ = 1.529 $W/m^2K$ | $a_{1A}$ = 1.771 $W/m^2K$ |
| $a_{2a}$ = 0.0166 $W/m^2K^2$ | $a_{2A}$ = 0.0192 $W/m^2K^2$ |

## B.2 Efficiency curve for the determined coefficients and for an assumed irradiation of 800 W/m$^2$ based on aperture area

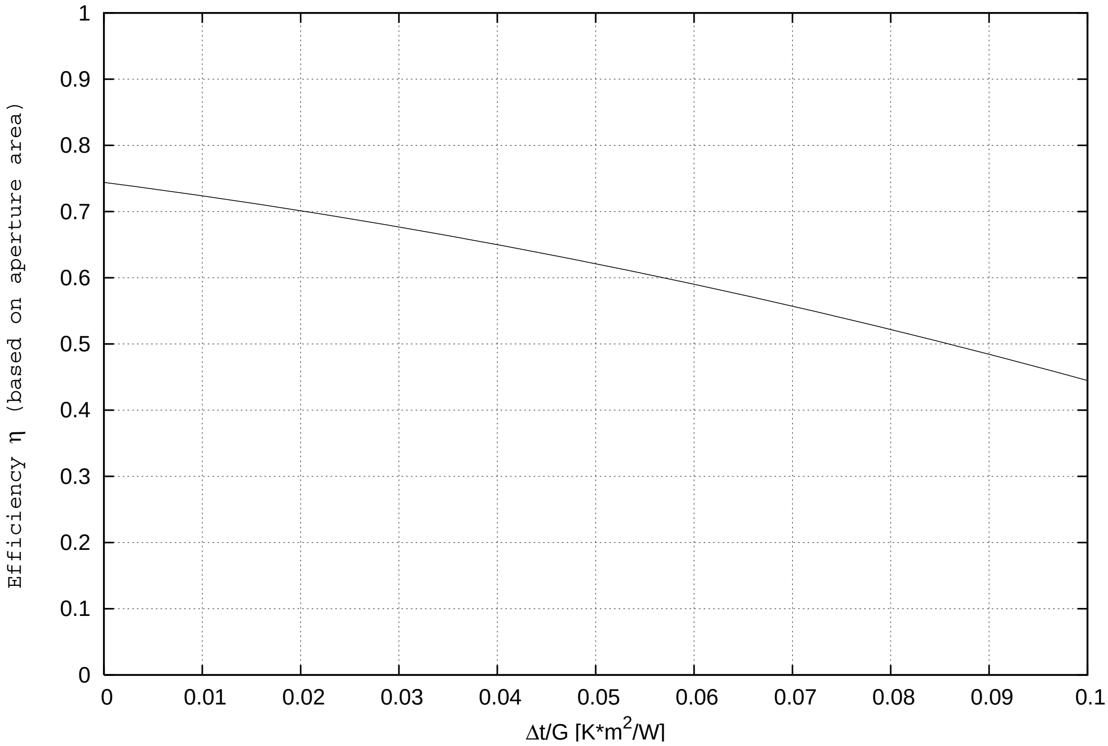


Figure 7: Efficiency curve scaled to 800 W/m$^2$ based on aperture area 0.936 m$^2$

The calculated parameters are based on following areas:

| aperture area: | absorber area: |
|---|---|
| $\eta_{0.05a}$ = 0.624 | $\eta_{0.05A}$ = 0.723 |

$\eta_{0.05}$ is the efficiency of the collector for typical conditions of solar domestic hot water systems:
irradiation of 800 W/m$^2$,
ambient temperature of 20 °C
mean collector temperture of 60 °C.

## B.3 Measured data for efficiency curve

| $G$ [W/m$^2$] | $G_d/G$ [-] | m [kg/h] | $t_{in}$ [°C] | $t_e$ [°C] | $t_e - t_{in}$ [K] | $t_m$ [°C] | $t_a$ [°C] | $t_m - t_a$ [K] | $(t_m - t_a)/G$ [K m$^2$/W] | $\eta_a$ [-] |
|---|---|---|---|---|---|---|---|---|---|---|
| 980 | 0.14 | 67.7 | 6.79 | 15.38 | 8.60 | 11.08 | 9.88 | 1.21 | 0.0012 | 0.740 |
| 992 | 0.13 | 67.7 | 6.81 | 15.46 | 8.65 | 11.14 | 9.88 | 1.26 | 0.0013 | 0.736 |
| 969 | 0.11 | 67.7 | 6.84 | 15.39 | 8.55 | 11.12 | 11.14 | -0.02 | -0.0000 | 0.745 |
| 937 | 0.09 | 67.8 | 7.78 | 16.05 | 8.27 | 11.91 | 11.05 | 0.86 | 0.0009 | 0.745 |
| 944 | 0.08 | 67.8 | 7.82 | 16.06 | 8.24 | 11.94 | 11.27 | 0.67 | 0.0007 | 0.737 |
| 852 | 0.17 | 60.8 | 6.76 | 15.14 | 8.38 | 10.95 | 10.39 | 0.56 | 0.0007 | 0.745 |
| 843 | 0.16 | 60.9 | 6.78 | 15.11 | 8.33 | 10.95 | 10.50 | 0.44 | 0.0005 | 0.749 |
| 892 | 0.12 | 66.1 | 33.03 | 40.28 | 7.25 | 36.66 | 7.43 | 29.23 | 0.0328 | 0.666 |
| 898 | 0.12 | 66.0 | 33.08 | 40.42 | 7.34 | 36.75 | 7.75 | 29.00 | 0.0323 | 0.669 |
| 905 | 0.12 | 66.1 | 33.10 | 40.52 | 7.42 | 36.81 | 7.97 | 28.84 | 0.0319 | 0.671 |
| 909 | 0.12 | 66.0 | 33.13 | 40.61 | 7.48 | 36.87 | 8.46 | 28.41 | 0.0312 | 0.673 |
| 916 | 0.12 | 65.8 | 33.15 | 40.69 | 7.54 | 36.92 | 8.56 | 28.36 | 0.0310 | 0.672 |
| 923 | 0.12 | 65.8 | 33.18 | 40.77 | 7.59 | 36.97 | 8.96 | 28.01 | 0.0304 | 0.671 |
| 921 | 0.12 | 65.9 | 33.26 | 40.87 | 7.61 | 37.07 | 9.85 | 27.21 | 0.0296 | 0.676 |
| 921 | 0.12 | 65.8 | 33.31 | 40.96 | 7.64 | 37.14 | 9.89 | 27.25 | 0.0296 | 0.678 |
| 919 | 0.12 | 65.9 | 33.36 | 41.00 | 7.64 | 37.18 | 10.33 | 26.85 | 0.0292 | 0.680 |
| 922 | 0.13 | 65.9 | 33.38 | 41.06 | 7.67 | 37.22 | 10.59 | 26.63 | 0.0289 | 0.680 |
| 967 | 0.09 | 66.6 | 60.04 | 67.08 | 7.04 | 63.56 | 11.76 | 51.80 | 0.0536 | 0.602 |
| 960 | 0.09 | 66.2 | 60.06 | 67.04 | 6.99 | 63.55 | 11.79 | 51.76 | 0.0539 | 0.599 |
| 944 | 0.09 | 66.3 | 60.04 | 66.97 | 6.93 | 63.50 | 11.58 | 51.92 | 0.0550 | 0.605 |
| 914 | 0.10 | 67.3 | 60.10 | 66.71 | 6.61 | 63.40 | 13.83 | 49.57 | 0.0543 | 0.604 |
| 931 | 0.10 | 65.7 | 85.10 | 90.63 | 5.53 | 87.87 | 6.87 | 80.99 | 0.0870 | 0.486 |
| 957 | 0.09 | 65.7 | 85.21 | 90.90 | 5.69 | 88.05 | 7.48 | 80.57 | 0.0842 | 0.488 |
| 980 | 0.08 | 65.6 | 85.47 | 91.43 | 5.97 | 88.45 | 7.81 | 80.64 | 0.0823 | 0.498 |
| 985 | 0.08 | 65.4 | 85.50 | 91.59 | 6.09 | 88.54 | 8.33 | 80.21 | 0.0815 | 0.504 |
| 987 | 0.08 | 64.9 | 85.57 | 91.66 | 6.09 | 88.61 | 8.92 | 79.69 | 0.0807 | 0.499 |
| 991 | 0.08 | 65.2 | 85.50 | 91.65 | 6.15 | 88.58 | 9.31 | 79.27 | 0.0800 | 0.504 |

Table 3: Data of measured efficiency points

# C Data of the exposure test

$H$: daily global irradiation

$valid\ period$: periods when the global irradiance $G$ is higher than 850 W/m$^2$ and the surrounding air temperature $t_a$ is higher than 10 °C

$t_a$: surrounding air temperature

$rain$: daily rain [mm]

| $Date$ | $H$ [MJ/m$^2$] | $valid\ period$ [h] | $t_a$ [°C] | $rain$ [mm] |
|---|---|---|---|---|
| 20061026 | 20.0 | 1.6 | 16.8 | 0 |
| 20061027 | 3.5 | 0.0 | 19.7 | 0 |
| 20061028 | 7.0 | 0.3 | 16.2 | 0 |
| 20061029 | 1.3 | 0.0 | 15.4 | 5 |
| 20061030 | 16.2 | 1.6 | 11.2 | 0 |
| 20061031 | 8.3 | 0.1 | 12.7 | 2 |
| 20061101 | 10.7 | 0.8 | 9.6 | 0 |
| 20061102 | 20.3 | 0.0 | 4.2 | 0 |
| 20061103 | 10.1 | 0.0 | 3.7 | 0 |
| 20061104 | 14.9 | 0.1 | 5.0 | 0 |
| 20061105 | 9.2 | 0.0 | 4.1 | 0 |
| 20061106 | 16.6 | 0.2 | 5.2 | 0 |
| 20061107 | 17.4 | 0.8 | 5.3 | 0 |
| 20061108 | 3.4 | 0.0 | 12.5 | 0 |
| 20061109 | 1.9 | 0.0 | 12.7 | 1 |
| 20061110 | 16.8 | 0.1 | 6.1 | 0 |
| 20061111 | 1.0 | 0.0 | 8.0 | 5 |
| 20061112 | 5.1 | 0.0 | 8.8 | 5 |
| 20061113 | 2.3 | 0.0 | 9.1 | 1 |
| 20061114 | 2.1 | 0.0 | 12.9 | 0 |
| 20061115 | 17.8 | 0.0 | 14.1 | 0 |
| 20061116 | 16.1 | 0.2 | 13.2 | 1 |
| 20061117 | 1.8 | 0.0 | 13.8 | 0 |
| 20061118 | 16.1 | 0.4 | 12.1 | 0 |
| 20061119 | 3.1 | 0.0 | 9.6 | 10 |
| 20061120 | 13.3 | 0.2 | 7.7 | 3 |
| 20061121 | 2.5 | 0.0 | 10.1 | 11 |
| 20061122 | 7.9 | 0.0 | 5.8 | 0 |
| 20061123 | 2.8 | 0.0 | 12.3 | 1 |
| 20061124 | 6.8 | 0.1 | 14.1 | 0 |
| 20061125 | 4.8 | 0.0 | 14.4 | 0 |
| 20061126 | 7.0 | 0.0 | 11.9 | 0 |
| 20061127 | 7.2 | 0.0 | 11.0 | 0 |
| 20061128 | 14.4 | 0.0 | 8.4 | 3 |
| 20061129 | 1.2 | 0.0 | 8.9 | 4 |
| 20061130 | 1.3 | 0.0 | 6.9 | 0 |

Continuation, see next page:

| *Date* | *H* [MJ/m²] | *valid period* [h] | $t_a$ [°C] | *rain* [mm] |
|---|---|---|---|---|
| 20061201 | 14.8 | 0.0 | 7.0 | 0 |
| 20061202 | 9.0 | 0.1 | 7.8 | 0 |
| 20061203 | 8.2 | 0.0 | 13.7 | 0 |
| 20061204 | 3.5 | 0.0 | 11.6 | 4 |
| 20061205 | 4.1 | 0.1 | 15.3 | 12 |
| 20061206 | 0.9 | 0.0 | 9.9 | 4 |
| 20061207 | 11.5 | 0.1 | 8.6 | 1 |
| 20061208 | 1.3 | 0.0 | 9.2 | 20 |
| 20061209 | 1.3 | 0.0 | 6.2 | 6 |
| 20061210 | 7.3 | 0.0 | 4.9 | 0 |
| 20061211 | 1.7 | 0.0 | 4.4 | 3 |
| 20061212 | 1.5 | 0.0 | 7.2 | 0 |
| 20061213 | 15.4 | 0.0 | 6.2 | 0 |
| 20061214 | 14.9 | 0.0 | 3.9 | 0 |
| 20061215 | 16.1 | 0.0 | 5.5 | 0 |
| 20061216 | 6.2 | 0.0 | 10.4 | 0 |
| 20061217 | 1.8 | 0.0 | 5.8 | 4 |
| 20061218 | 9.2 | 0.0 | 2.3 | not spezified |
| 20061219 | 13.9 | 0.0 | 3.1 | not spezified |
| 20061220 | 15.5 | 0.0 | 2.1 | not spezified |
| 20061221 | 15.7 | 0.0 | 2.0 | not spezified |
| 20061222 | 14.4 | 0.0 | 2.0 | not spezified |
| 20061223 | 0.9 | 0.0 | -1.3 | not spezified |
| 20061224 | 1.0 | 0.0 | 0.1 | not spezified |
| 20061225 | 0.6 | 0.0 | -0.9 | not spezified |
| 20061226 | 1.1 | 0.0 | -0.9 | not spezified |
| 20061227 | 9.4 | 0.0 | -1.7 | not spezified |
| 20061228 | 11.0 | 0.0 | -1.5 | not spezified |
| 20061229 | 12.3 | 0.0 | 1.4 | not spezified |
| 20061230 | 5.0 | 0.0 | 5.8 | not spezified |
| 20061231 | 9.3 | 0.0 | 12.0 | not spezified |
| 20070101 | 1.6 | 0.0 | 10.9 | not spezified |
| 20070102 | 2.0 | 0.0 | 4.7 | not spezified |
| 20070103 | 3.7 | 0.0 | 5.5 | not spezified |
| 20070104 | 1.0 | 0.0 | 7.4 | not spezified |
| 20070105 | 1.1 | 0.0 | 7.5 | not spezified |
| 20070106 | 1.7 | 0.0 | 10.1 | not spezified |
| 20070107 | 2.5 | 0.0 | 9.8 | not spezified |
| 20070108 | 1.0 | 0.0 | 10.8 | not spezified |
| 20070109 | 1.5 | 0.0 | 12.6 | not spezified |
| 20070110 | 13.4 | 0.0 | 13.5 | not spezified |

Continuation, see next page:

| *Date* | *H* [MJ/m²] | *valid period* [h] | $t_a$ [°C] | *rain* [mm] |
|---|---|---|---|---|
| 20070111 | 5.6 | 0.0 | 10.3 | not spezified |
| 20070112 | 4.1 | 0.0 | 9.3 | not spezified |
| 20070113 | 17.0 | 0.1 | 10.7 | not spezified |
| 20070114 | 4.3 | 0.1 | 9.1 | not spezified |
| 20070115 | 2.4 | 0.0 | 2.2 | not spezified |
| 20070116 | 3.0 | 0.0 | 6.2 | not spezified |
| 20070117 | 1.8 | 0.0 | 11.0 | not spezified |
| 20070118 | 0.3 | 0.0 | 13.1 | not spezified |
| 20070119 | 1.5 | 0.0 | 12.8 | not spezified |
| 20070120 | 7.6 | 0.2 | 12.7 | not spezified |
| 20070121 | 9.6 | 0.1 | 8.9 | not spezified |
| 20070122 | 2.1 | 0.0 | 4.6 | not spezified |
| 20070123 | 0.8 | 0.0 | 0.4 | not spezified |
| 20070124 | 1.7 | 0.0 | -4.4 | not spezified |
| 20070125 | 3.6 | 0.0 | -5.3 | not spezified |
| 20070126 | 19.2 | 0.0 | -4.1 | not spezified |
| 20070127 | 2.0 | 0.0 | -0.6 | not spezified |
| 20070128 | 16.5 | 0.0 | 2.9 | not spezified |
| 20070129 | 2.1 | 0.0 | 4.3 | not spezified |
| 20070130 | 18.1 | 0.0 | 3.5 | not spezified |
| 20070131 | 3.0 | 0.0 | 2.0 | not spezified |
| 20070201 | 4.0 | 0.0 | 3.6 | 0 |
| 20070202 | 18.0 | 0.0 | 4.7 | 0 |
| 20070203 | 19.5 | 0.0 | 6.3 | 0 |
| 20070204 | 21.0 | 0.7 | 5.0 | 1 |
| 20070205 | 6.5 | 0.0 | 5.9 | 5 |
| 20070206 | 0.8 | 0.0 | 3.6 | 1 |
| 20070207 | 1.6 | 0.0 | 5.0 | 4 |
| 20070208 | 2.5 | 0.0 | 7.5 | 6 |
| 20070209 | 18.9 | 1.7 | 8.0 | 3 |
| 20070210 | 2.3 | 0.0 | 7.7 | 3 |
| 20070211 | 5.0 | 0.7 | 8.8 | 3 |
| 20070212 | 1.6 | 0.0 | 9.3 | 5 |
| 20070213 | 2.9 | 0.0 | 7.2 | 0 |
| 20070214 | 1.5 | 0.0 | 5.5 | 12 |
| 20070215 | 16.5 | 1.6 | 8.3 | 0 |
| 20070216 | 20.6 | 1.7 | 5.3 | 0 |
| 20070217 | 11.2 | 0.0 | 4.9 | 0 |

Continuation, see next page:

| *Date* | $H$ [MJ/m$^2$] | *valid period* [h] | $t_a$ [°C] | *rain* [mm] |
|---|---|---|---|---|
| 20070218 | 19.4 | 1.6 | 6.4 | 0 |
| 20070219 | 14.9 | 0.0 | 5.5 | 0 |
| 20070220 | 13.0 | 0.0 | 3.1 | 0 |
| 20070221 | 21.1 | 2.6 | 7.3 | 0 |
| 20070222 | 18.6 | 0.4 | 11.2 | 0 |
| 20070223 | 16.3 | 1.1 | 11.7 | 6 |
| 20070224 | 4.0 | 0.0 | 10.7 | 5 |
| 20070225 | 4.2 | 0.0 | 8.9 | 3 |
| 20070226 | 3.1 | 0.0 | 6.9 | 5 |
| 20070227 | 7.1 | 0.0 | 6.7 | 2 |
| 20070228 | 6.6 | 0.2 | 10.9 | 2 |
| 20070301 | 1.9 | 0.0 | 9.4 | 0 |
| 20070302 | 11.3 | 0.1 | 8.1 | 0 |
| 20070303 | 12.7 | 1.7 | 12.0 | 0 |
| 20070304 | 23.7 | 4.0 | 11.2 | 0 |
| 20070305 | 9.1 | 0.1 | 10.3 | 0 |
| 20070306 | 9.8 | 0.4 | 9.5 | 0 |
| 20070307 | 8.9 | 0.5 | 10.3 | 0 |
| 20070308 | 20.8 | 3.5 | 8.4 | 0 |
| 20070309 | 14.8 | 0.8 | 7.6 | 0 |
| 20070310 | 22.2 | 1.1 | 6.7 | 0 |
| 20070311 | 25.7 | 2.6 | 7.4 | 0 |
| 20070312 | 25.5 | 3.6 | 8.6 | 0 |
| 20070313 | 23.6 | 3.0 | 10.1 | 0 |
| 20070314 | 21.3 | 2.3 | 9.5 | 0 |

# Thermistor Elements

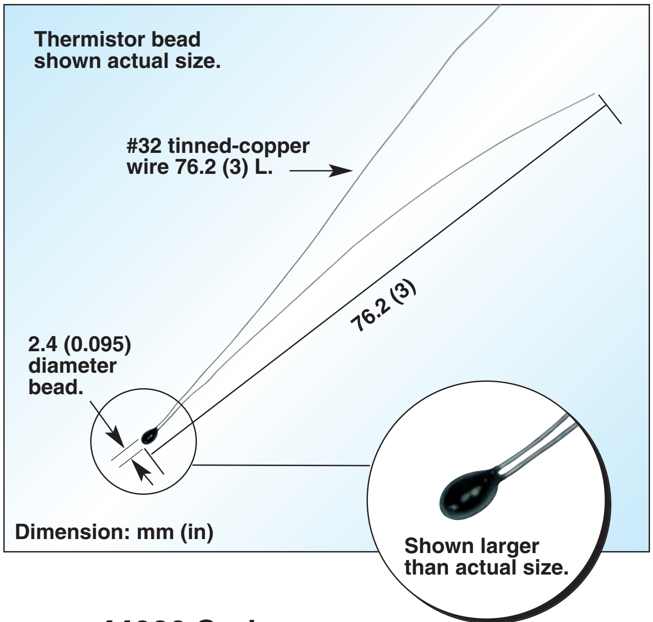


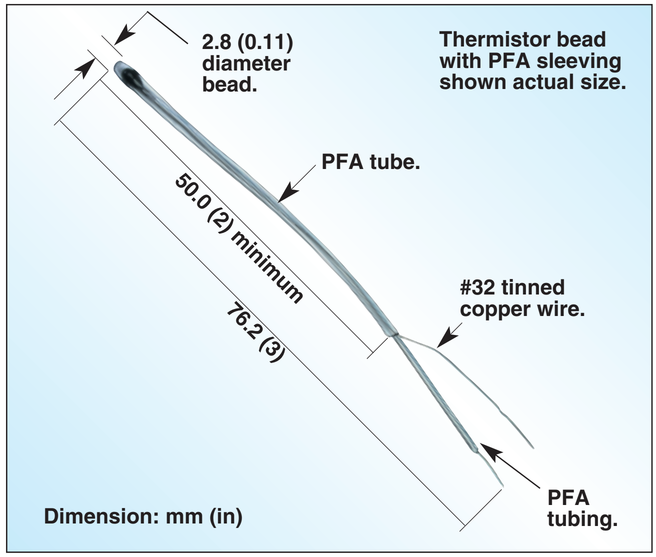


**44000 Series Starts at $15**

RoHS

- **Epoxy Coated Thermistor Beads**
- **Precision Matched to 5 Standardized Resistance Curves**
- **Maximum Working Temperature 75°C (165°F) or 150°C (300°F) (See Table Below)**
- **Available in Interchangeabilities of ±0.1 or ±0.2°C (See Table Below)**

### Resistance Vs. Temperature Characteristics

The Steinhart-Hart Equation has become the generally accepted method for specifying the resistance vs. temperature characteristics for thermistors. The Steinhart-Hart equation for temperature as a function of resistance is as follows:

$\frac{1}{T} = A + B\,[\mathrm{Ln}(R)] + C\,[\mathrm{Ln}(R)]^3$

where: A, B and C are constants derived from 3 temperature test points.
R = Thermistor's resistance in Ω
T = Temperature in degrees K

To determine the thermistor resistance at a specific temperature point, the following equation is used:

$R = e^{(beta-(alpha/2))1/3 - ((beta+(alpha/2))1/3}$

where:
alpha = ((A-(1/T))/C)
beta = SQRT(((B/(3C))$^3$)+(alpha$^2$/4))
T = Temperature in Kelvin (°C + 273.15)

The A, B and C constants for each of our thermistor selections can be found in Table 1. Using these constants with the above equations, you can determine the temperature of the thermistor based on its resistance, or determine a thermistor's resistance at a particular temperature.

**Typical Thermometric Drift (±0.2°C Elements)**

| Operating Temp | 10 Months | 100 Months |
|---|---|---|
| 0°C | <0.01°C | <0.01°C |
| 25°C | <0.01°C | 0.02°C |
| 100°C | 0.20°C | 0.32°C |
| 150°C | 1.5°C | Not recommended |

**Table 1: Steinhart-Hart Constants**

| Model Number | Model Number | R25°C | A | B | C |
|---|---|---|---|---|---|
| **44004** | **44033** | **2252** | $1.468 \times 10^{-3}$ | $2.383 \times 10^{-4}$ | $1.007 \times 10^{-7}$ |
| **44005** | **44030** | **3000** | $1.403 \times 10^{-3}$ | $2.373 \times 10^{-4}$ | $9.827 \times 10^{-8}$ |
| **44007** | **44034** | **5000** | $1.285 \times 10^{-3}$ | $2.362 \times 10^{-4}$ | $9.285 \times 10^{-8}$ |
| **44006** | **44031** | **10000** | $1.032 \times 10^{-3}$ | $2.387 \times 10^{-4}$ | $1.580 \times 10^{-7}$ |
| **44008** | **44032** | **30000** | $9.376 \times 10^{-4}$ | $2.208 \times 10^{-4}$ | $1.276 \times 10^{-7}$ |

### Tolerance Curves

Accuracy tolerances for thermistor sensors are expressed as a percentage of temperature. This is also referred to as interchangeability. We list two basic accuracy/interchangeability specifications for our thermistors, ±0.10°C and ±0.20°C from 0 to 70°C (32 to 158°F).

**Table 2: Interchangeability Tolerances**

| Temp (°C) | Model No. 44004 ±0.20°C | | Model No. 44033 ±0.10°C | |
|---|---|---|---|---|
| | ±°C | ±Ω | ±°C | ±Ω |
| -80 | 1.00 | 142,000 | 1.00 | 142,000 |
| -40 | 0.40 | 2018 | 0.20 | 1009 |
| 0 | 0.20 | 75 | 0.10 | 38 |
| 40 | 0.20 | 10 | 0.10 | 4.9 |
| 70 | 0.20 | 2.7 | 0.10 | 1.4 |
| 100 | 0.30 | 1.3 | 0.15 | 0.7 |
| 150 | 1.00 | 0.9 | 1.00 | 0.9 |

***Note:*** *Temperature values (°C) are the same for each tolerance group (±0.10 or ±0.20), resistance tolerances will change based on resistance at 25°C (77°F).*

Temperature vs. resistance tables for our thermistor products can be found on pages Z-236 and Z-237. The accuracy specification of ±0.1% or 0.2% means that each thermistor's resistance will fall within these limits between 0 and 70°C (32 and 158°F).
Table 2 illustrates the interchangeability values for the model numbers 44004 (±0.2°C) and 44033 (±0.1°C) at a number of temperatures.

### Stability and Drift

While thermistors are generally very accurate and stable devices, conditions such as over-temperature exposure, humidity, mechanical damage or corrosion can cause uncontrolled changes in the resistance vs. temperature characteristics of the device. Once this characteristic has been altered, it cannot be re-established. This is one reason why most thermistors with a ±0.1°C interchangeability specifcation are rated for use at temperatures somewhat lower than those with an interchangeability of ±0.2°C.

### Operating Current

The suggested operating current for bead-style thermistors is approximately 10 to 15 µA. Thermistors can experience self-heating effects if their operating currents are high enough to create more heat than can be dissipated from the thermistor under operating conditions. If higher operating currents are used, it is suggested that a self heating test be performed to insure the accuracy of the measurement.

### Dissipation Constant

The dissipation constant is the power in milliwatts that will raise the resistance of a thermistor by 1°C (1.8°F) over its surrounding temperature. Typical values include 8 mW/°C in a stirred oil bath, or 1 mW/°C in still air.

### Time Constant

The time constant is the time required for a thermistor to react to a step change in temperature. For example, if exposed to a change from 0 to 100°C (32 to 212°F), the 63% time constant would be the time required for the thermistor to indicate a resistance at 63°C (145°F). Typically, bare thermistors suspended by their leads in a well stirred oil bath will have a 63% response time of 1 second maximum. PFA encased thermistors exposed to changes in air temperature will typically have a 63% response time of 2.5 seconds maximum.

| Discount Schedule | |
|---|---|
| 1 to 9 | Net |
| 10 to 24 | 10% |
| 25 to 49 | 20% |
| 50 to 99 | 30% |
| 100 and over | 40% |

D

***MOST POPULAR MODELS HIGHLIGHTED!***

## To Order *(Specify Model Number)*

| Model Number | Price (Each) | Resistance @ 25°C (Ω) | Maximum Working Temp | Interchangeability @ 0 to 70°C | Storage and Working Temp for Best Stability |
|---|---|---|---|---|---|
| **44004** | **$15** | 2252 | 150°C (300°F) | ±0.2°C | -80 to 120°C (-110 to 250°F) |
| **44005** | **15** | 3000 | 150°C (300°F) | ±0.2°C | -80 to 120°C (-110 to 250°F) |
| **44007** | **15** | 5000 | 150°C (300°F) | ±0.2°C | -80 to 120°C (-110 to 250°F) |
| **44006** | **15** | 10,000 | 150°C (300°F) | ±0.2°C | -80 to 120°C (-110 to 250°F) |
| **44008** | **15** | 30,000 | 150°C (300°F) | ±0.2°C | -80 to 120°C (-110 to 250°F) |
| **44033** | **$22** | 2252 | 75°C (165°F) | ±0.1°C | -80 to 75°C (-110 to 165°F) |
| **44030** | **22** | 3000 | 75°C (165°F) | ±0.1°C | -80 to 75°C (-110 to 165°F) |
| **44034** | **22** | 5000 | 75°C (165°F) | ±0.1°C | -80 to 75°C (-110 to 165°F) |
| **44031** | **22** | 10,000 | 75°C (165°F) | ±0.1°C | -80 to 75°C (-110 to 165°F) |
| **44032** | **22** | 30,000 | 75°C (165°F) | ±0.1°C | -80 to 75°C (-110 to 165°F) |

***Note:*** *Thermistor elements are available with PFA sleeving over 1 lead wire and PFA overall, change middle digit model number to **"1"** and add **$24** to the base price for the ±0.2°C thermistors and add **$49** for the price of the ± 0.1°C thermistors.*

***Ordering Examples: 44004,*** *2252 Ω thermistor bead at 25°C, ±0.2°C interchangeability, **$15. 44033,** 2252 Ω thermistor bead at 25°C, ±0.1°C interchangeability, **$22.***

***44104,*** *2252 Ω thermistor bead at 25°C, ±0.2°C interchangeability with PFA insulated lead wire and over-jacket, $15 + 24 = **$39.***

***44033,*** *2252 Ω thermistor bead at 25°C, ±0.1°C interchangeability with PFA insulated lead wire and over-jacket, $22 + 49 = **$71.***

# omega.com®

*Your One-Stop Source for Process Measurement and Control!*

**One Omega Drive | Stamford, CT 06907 | 1-888-TC-OMEGA (1-888-826-6342) | info@omega.com**

**www.omega.com**

**UNITED STATES**
www.omega.com
1-800-TC-OMEGA
Stamford, CT.

**CANADA**
www.omega.ca
Laval(Quebec)
1-800-TC-OMEGA

**GERMANY**
www.omega.de
Deckenpfronn, Germany
0800-8266342

**UNITED KINGDOM**
www. omega.co.uk
Manchester, England
0800-488-488

**FRANCE**
www.omega.fr
Guyancourt, France
088-466-342

**CZECH REPUBLIC**
www.omegaeng.cz
Karviná, Czech Republic
596-311-899

**BENELUX**
www.omega.nl
Amstelveen, NL
0800-099-33-44

# *More than 100,000 Products Available!*

## • Temperature

Calibrators, Connectors, General Test and Measurement Instruments, Glass Bulb Thermometers, Handheld Instruments for Temperature Measurement, Ice Point References, Indicating Labels, Crayons, Cements and Lacquers, Infrared Temperature Measurement Instruments, Recorders Relative Humidity Measurement Instruments, RTD Probes, Elements and Assemblies, Temperature & Process Meters, Timers and Counters, Temperature and Process Controllers and Power Switching Devices, Thermistor Elements, Probes and Assemblies, Thermocouples Thermowells and Head and Well Assemblies, Transmitters, Wire

## • Flow and Level

Air Velocity Indicators, Doppler Flowmeters, Level Measurement, Magnetic Flowmeters, Mass Flowmeters, Pitot Tubes, Pumps, Rotameters, Turbine and Paddle Wheel Flowmeters, Ultrasonic Flowmeters, Valves, Variable Area Flowmeters, Vortex Shedding Flowmeters

## • pH and Conductivity

Conductivity Instrumentation, Dissolved Oxygen Instrumentation, Environmental Instrumentation, pH Electrodes and Instruments, Water and Soil Analysis Instrumentation

## • Data Acquisition

Auto-Dialers and Alarm Monitoring Systems, Communication Products and Converters, Data Acquisition and Analysis Software, Data Loggers Plug-in Cards, Signal Conditioners, USB, RS232, RS485 and Parallel Port Data Acquisition Systems, Wireless Transmitters and Receivers

## • Pressure, Strain and Force

Displacement Transducers, Dynamic Measurement Force Sensors, Instrumentation for Pressure and Strain Measurements, Load Cells, Pressure Gauges, Pressure Reference Section, Pressure Switches, Pressure Transducers, Proximity Transducers, Regulators, Strain Gages, Torque Transducers, Valves

## • Heaters

Band Heaters, Cartridge Heaters, Circulation Heaters, Comfort Heaters, Controllers, Meters and Switching Devices, Flexible Heaters, General Test and Measurement Instruments, Heater Hook-up Wire, Heating Cable Systems, Immersion Heaters, Process Air and Duct, Heaters, Radiant Heaters, Strip Heaters, Tubular Heaters

**• *click here to go to the omega.com home page* •**

# LONG-LIFE PULSE OUTPUT WATER METERS

## For Remote Rate Indication and Totalization

**FTB4600 Series**
**Starts at**
**$180**

1 YEAR WARRANTY

- For Water Flows from 0.15 to 20 GPM
- Economical
- High Turndown Ratio
- Up to ±1.5% Rdg Accuracy

**FTB4605 pulse output water meter, $180, shown smaller than actual size.**

**Comes complete with built-in strainers, locking nuts, gaskets, coupling pieces, 1.5 m (5') cable and operator's manual.**

Designed for long-term water billing applications, the FTB4600 Series flowmeters are highly accurate and feature a high-frequency pulse output suitable for remote flow-rate indication or flow totalization. For economy, they have no local indication of the flow rate or total. The pulse output is compatible with OMEGA's DPF400 and DPF700 Series ratemeter/totalizers. All meters come with built-in strainers, locking nuts, gaskets, coupling pieces, and 1.5 m (5') of 3-conductor copper wire.

### SPECIFICATIONS

**Accuracy:** From 10% of continuous to max flow: ±1.5% of rate; below 10% of continuous flow: 2% of rate
**Fluid Temperature Range:** 0 to 88°C (32 to 190°F)
**Wetted Parts:** Brass body, stainless steel, polyimide (fiberglass), polypropylene, EPDM O-ring
**Pressure Drop (at Continuous Flow Rate):** 2.9 psid
**Max Pressure:** 150 psig
**Pulse Output:** Requires 6 to 16 Vdc @ 10 mA max power; output requires pull-up to positive DC voltage; includes 1.5 m (5') of cable
**Duty Cycle:** 50-50


**DPF700 Series ratemeter/totalizer/ batch controller, $260.** **See page M-5.**


F

***AVAILABLE FOR FAST DELIVERY!***

## To Order *(Specify Model Number)*

**Bronze Body**

| Model No. | Price | Port Size | Flow Rate (GPM) | | | Dimensions: mm (in) | | | Weight kg (lb) | Pulses per Gallon |
|---|---|---|---|---|---|---|---|---|---|---|
| | | | Min | Cont. | Max | Length | Height | Width | | |
| **FTB4605** | **$180** | ½" | 0.15 | 6.6 | 13.0 | 110 (4.3) | 70 (2.75) | 70 (2.75) | 0.5 (1.1) | 151.4 |
| **FTB4607** | **200** | ¾" | 0.22 | 11.0 | 20.0 | 130 (5.13) | 73 (2.9) | 70 (2.75) | 0.6 (1.4) | 75.7 |
| **FW-0119** | **160** | Reference Book: Flow Measurement | | | | | | | | |

*Comes complete with built-in strainers, locking nuts, gaskets, coupling pieces, 1.5 m (5') cable and operator's manual.*
***Ordering Examples: FTB4605,** bronze body water meter, ½" port size, **$180.***
***FTB4607**, bronze body water meter, ¾" port size, **$200.***

# omega.com®

*Your One-Stop Source for Process Measurement and Control!*

**One Omega Drive | Stamford, CT 06907 | 1-888-TC-OMEGA (1-888-826-6342) | info@omega.com**

**www.omega.com**

**UNITED STATES**
www.omega.com
1-800-TC-OMEGA
Stamford, CT.

**CANADA**
www.omega.ca
Laval(Quebec)
1-800-TC-OMEGA

**GERMANY**
www.omega.de
Deckenpfronn, Germany
0800-8266342

**UNITED KINGDOM**
www. omega.co.uk
Manchester, England
0800-488-488

**FRANCE**
www.omega.fr
Guyancourt, France
088-466-342

**CZECH REPUBLIC**
www.omegaeng.cz
Karviná, Czech Republic
596-311-899

**BENELUX**
www.omega.nl
Amstelveen, NL
0800-099-33-44

# *More than 100,000 Products Available!*

- ## Temperature

Calibrators, Connectors, General Test and Measurement Instruments, Glass Bulb Thermometers, Handheld Instruments for Temperature Measurement, Ice Point References, Indicating Labels, Crayons, Cements and Lacquers, Infrared Temperature Measurement Instruments, Recorders Relative Humidity Measurement Instruments, RTD Probes, Elements and Assemblies, Temperature & Process Meters, Timers and Counters, Temperature and Process Controllers and Power Switching Devices, Thermistor Elements, Probes and Assemblies, Thermocouples Thermowells and Head and Well Assemblies, Transmitters, Wire

- ## Flow and Level

Air Velocity Indicators, Doppler Flowmeters, Level Measurement, Magnetic Flowmeters, Mass Flowmeters, Pitot Tubes, Pumps, Rotameters, Turbine and Paddle Wheel Flowmeters, Ultrasonic Flowmeters, Valves, Variable Area Flowmeters, Vortex Shedding Flowmeters

- ## pH and Conductivity

Conductivity Instrumentation, Dissolved Oxygen Instrumentation, Environmental Instrumentation, pH Electrodes and Instruments, Water and Soil Analysis Instrumentation

- ## Data Acquisition

Auto-Dialers and Alarm Monitoring Systems, Communication Products and Converters, Data Acquisition and Analysis Software, Data Loggers Plug-in Cards, Signal Conditioners, USB, RS232, RS485 and Parallel Port Data Acquisition Systems, Wireless Transmitters and Receivers

- ## Pressure, Strain and Force

Displacement Transducers, Dynamic Measurement Force Sensors, Instrumentation for Pressure and Strain Measurements, Load Cells, Pressure Gauges, Pressure Reference Section, Pressure Switches, Pressure Transducers, Proximity Transducers, Regulators, Strain Gages, Torque Transducers, Valves

- ## Heaters

Band Heaters, Cartridge Heaters, Circulation Heaters, Comfort Heaters, Controllers, Meters and Switching Devices, Flexible Heaters, General Test and Measurement Instruments, Heater Hook-up Wire, Heating Cable Systems, Immersion Heaters, Process Air and Duct, Heaters, Radiant Heaters, Strip Heaters, Tubular Heaters

**• *click here to go to the omega.com home page* •**